NASA TECHNICAL NOTE

NASA TN D-8190

NASA TN D-8190

A SIMULATION STUDY OF CURVED, DESCENDING, DECELERATING, LANDING APPROACHES FOR TRANSPORT AIRCRAFT

James E. Dieudonne, Randall D. Grove, and George G. Steinmetz

Langley Research Center
Hampton, Va. 23665

NATIONAL AERONAUTICS AND SPACE ADMINISTRATION • WASHINGTON, D. C. • APRIL 1976

1. Report No.	2. Government Accession No.	3. Recip
NASA TN D-8190		

4. Title and Subtitle
A SIMULATION STUDY OF CURVED, DESCENDING, DECELERATING, LANDING APPROACHES FOR TRANSPORT AIRCRAFT

5. Report Date
April 1976

6. Performing Organization Code
L-10584

7. Author(s)
James E. Dieudonne, Randall D. Grove, and George G. Steinmetz

8. Performing Organization Report No.

9. Performing Organization Name and Address
NASA Langley Research Center
Hampton, Va. 23665

10. Work Unit No.
513-52-01-18

11. Contract or Grant No.

12. Sponsoring Agency Name and Address
National Aeronautics and Space Administration
Washington, D.C. 20546

13. Type of Report and Period Covered
Technical Note

14. Sponsoring Agency Code

15. Supplementary Notes

16. Abstract

During recent years the problems of congestion, noise pollution, and safety in the vicinity of airports have indicated that changes must be made in the operational aspects of aircraft landing approaches. Suggested changes include curved approaches, steep approaches, decelerating approaches, and combinations of these. This paper describes a system which is capable of controlling an aircraft automatically along a curved, descending, decelerating approach. A simulation study was conducted to determine the necessary modifications to the basic flight-proven control system. This basic system is presently being used to accomplish straight-in automatic landing approaches on a short-haul transport aircraft (B-737 terminal configured vehicle). This study shows that both 3^{o} (normal) and 5^{o} (steep) approaches could be accomplished with only minor modifications to the basic control system.

17. Key Words (Suggested by Author(s))
Automatic landing
Curved approach
Decelerating approach

18. Distribution Statement
Unclassified – Unlimited

Subject Category 08

19. Security Classif. (of this report)	20. Security Classif. (of this page)	21. No. of Pages	22. Price*
Unclassified	Unclassified	41	$3.75

*For sale by the National Technical Information Service, Springfield, Virginia 22161

A SIMULATION STUDY OF CURVED, DESCENDING, DECELERATING, LANDING APPROACHES FOR TRANSPORT AIRCRAFT

James E. Dieudonne, Randall D. Grove,
and George G. Steinmetz
Langley Research Center

SUMMARY

During recent years the problems of congestion, noise pollution, and safety in the vicinity of airports have indicated that changes must be made in the operational aspects of aircraft landing approaches. Suggested changes include curved approaches, steep approaches, decelerating approaches, and combinations of these. This paper describes a system which is capable of controlling an aircraft automatically along a curved, descending, decelerating approach. A simulation study was conducted to determine the necessary modifications to the basic flight-proven control system. This basic system is presently being used to accomplish straight-in automatic landing approaches on a short-haul transport aircraft (B-737 terminal configured vehicle). This study shows that both 3° (normal) and 5° (steep) approaches could be accomplished with only minor modifications to the basic control system.

INTRODUCTION

Aircraft operations in the terminal area have been the topic of many studies in recent years. The increased traffic in the terminal area and the projected further increase in the future require that changes in terminal area operations be made. At present, aircraft are usually vectored along straight-line paths to a common point; the aircraft are then sequenced to follow each other down a shallow flight path for a straight-in approach to the runway. Present procedures also dictate that the entire final approach be flown at the desired landing speed and in a landing configuration.

As pointed out in reference 1, these paths often result in low-altitude flying over densely populated areas at relatively high power settings. The additional noise pollution and the safety hazards of flying at low altitudes make the procedure objectionable. Steeper flight paths and two-segment final approaches (ref. 1) have been proposed as solutions to these problems. Curved approaches (refs. 2, 3, and 4) have also been proposed as an alternative to these procedures. The steep curved approach has certain advantages: it keeps the aircraft at relatively high altitude, except in the immediate area of the airport,

and it routes traffic away from densely populated areas. A deceleration to landing speed during the final approach has also been recommended (ref. 5) as an aid in the reduction of noise pollution. This paper proposes a steep-curve, decelerating final approach which combines all the advantages of the flight paths recommended earlier.

The paper describes the design of a system to control an aircraft along this approach. This design is a modification of a flight-proved inertially augmented automatic landing system designed to accomplish a straight-in approach using the standard instrument landing system (ILS). The unmodified or basic system is documented in references 6 and 7 and is presently being flown on the B-737 aircraft as part of the terminal configured vehicle (TCV) program.

The paper describes a simulation study which investigated the design of a system capable of controlling an aircraft along a curved, descending, decelerating path. The simulation of the B-737 is very complete in that it contains a nonlinear aerodynamics package together with realistic representations of onboard avionics, guidance and control systems, and actuators; such realism enhances confidence in the results obtained. Results are presented for the curved decelerating approaches along both 3° and 5° glide paths. The tests included the simulation of turbulence, winds, and noise representing very high frequency omnirange and microwave landing system errors.

SYMBOLS

A_c acceleration error signal, m/sec^2

C_{knob} knob input for V_c, knots

D_{tg} path distance to threshold, m

GSA glide-slope angle, deg

GSE glide-slope error, deg

g gravity, m/sec^2

h radio altitude, m

K_d 1/100 of desired glide-slope angle (0.03 and 0.05)

K_t tangent of glide-slope angle to be flown (0.0524 and 0.0875)

ℓ_{gt} distance of glide-slope location from runway threshold, m

ℓ_r	length of runway, m
ℓ_{t3}	distance between runway threshold and point 3, m
q	body pitch rate, deg/sec
R	radius of turn, m
S_p	flight spoiler position, deg
s	Laplace operator
t	time, sec
$\dot{V}'$	autothrottle wind shear compensation command, m/sec^2
V_c	calibrated airspeed, knots
V_{cd}	desired calibrated airspeed, knots
V_g	groundspeed, m/sec
V_i	indicated airspeed, knots
V_t	true airspeed, m/sec
V_y	crosstrack velocity, m/sec
X_R,Y_R,Z_R	local coordinate system
X_T,Y_T,Z_T	turn center coordinate system
x,y,z	aircraft position relative to local coordinate system
x_{AT},y_{AT},z_{AT}	aircraft position relative to turn center coordinate system
α	aircraft angle of attack, deg
β	angle for determining flight-path segment, deg

γ	flight-path angle, deg
$\Delta h, \Delta y$	vertical and lateral errors from path, m
$\Delta h_{nor}, \Delta y_{nor}$	normalization variables for glide-slope and localizer error signals, m
$\Delta\psi_c$	decrab command to aileron, deg
$\Delta\psi_{tr}$	track-angle error between aircraft and path, deg
δ_{ac}	aileron command, deg
δ_{ec}	elevator command, deg
δ_{eg}	glide-slope error command, deg
δ_F	flap position, deg
δ_{rc}	rudder command, deg
δ_t	commanded change in throttle position, deg
η	localizer error signal, deg
η_ℓ	variable limit on localizer error signal
θ	pitch attitude, deg
ϕ	roll angle, deg
ϕ_c	roll-angle command, deg
ϕ_{er}	roll-angle error, deg
ϕ_{ILS}	lateral error signal, deg
ϕ_{nom}	nominal bank angle (curved path), deg
$\dot{\phi}_{limit}$	roll rate limit, deg/sec

ψ aircraft heading, deg

ψ_r path heading, deg

ψ_t aircraft track angle, deg

Abbreviations:

AGCS automatic guidance and control system

DME distance measuring equipment

HDG runway heading

HPC horizontal path command

ILS instrument landing system

INS inertial navigation system

MLS microwave landing system

ONCOR on-course logic

RSFS research support flight system

TCV terminal configured vehicle

VOR very high frequency omnirange

VPC vertical path command

A dot over a symbol denotes a time derivative; the symbol | | denotes an absolute value.

DESCRIPTION OF SIMULATION

This study was conducted by use of a simulation of the research support flight system (RSFS) described in reference 8. The simulation was conducted on the real-time

simulation subsystem (ref. 9) at the Langley Research Center; the simulation included a representation of the major components shown in figure 1.

The aircraft mathematical model was a representation of a B-737 aircraft. The model included a nonlinear data package for all flight regions, a nonlinear engine model, and nonlinear models of servos, actuators, spoiler mixers, and other associated flight hardware. The simulation of the basic airframe was verified as realistic by comparing simulation data with actual aircraft response data and by pilot evaluation. Approximations of VOR, DME, and MLS models were used.

The functions of the navigation-guidance and flight control computers are shown in more detail in figure 2 and are described in references 6 and 7. A complete representation of all the flight control systems (control wheel steering, navigation, autoland) and associated logic is in the simulation. The mode of the simulation is controlled by the AGCS mode select panel. Inputs to the navigation computer are made by the navigation control and display unit (NCDU) from which the flight plan can be initiated or altered. (The NCDU was not used in this study.)

The primary displays include an electronic attitude direction indicator (EADI) and an electronic horizontal situation indicator (EHSI). These displays are generated by an Adage graphic system and are sent by closed circuit television to the cockpit to be displayed on cathode ray tubes. These displays were not necessary for this particular study. The displays were used as monitoring devices and were included to show the totality of the simulation.

FLIGHT-PATH DESCRIPTION

The approach path is shown in figure 3 and can be defined by the navigation-guidance equations in reference 6. These navigation equations were modified to meet the requirements of the autoland control system for this flight path. The functional aspects of the path are: (1) a deceleration from 200 knots to an approach speed of 120 knots requiring automatic deployment of flaps, flight spoilers, and actuation of the throttles; (2) a constant radius turn with a heading change of 180^{o}; (3) a short (1524 m) final leg to threshold; and (4) a steep, constant descent during the entire approach.

The flight path was divided into segments, and logic was developed to determine the particular segment as a function of the current aircraft position. The required aircraft position (x,y,z) was determined relative to a local coordinate system. The local coordinate system $\left(X_R,Y_R,Z_R\right)$ chosen for this study was located at the threshold of the runway and was oriented as shown in figure 3. During the study, it was assumed that the aircraft position (x,y,z) was obtained by regular radio navigation means from point 0 to point 1

and by MLS from point 1 to touchdown. Initial offsets of the aircraft from the path at point 0 represent errors in reaching the flight path by other means.

The origin of the turn center coordinate system (X_T, Y_T, Z_T) was located at the center of the turn and was oriented as shown in figure 3. The aircraft position relative to this coordinate system is calculated as

$$x_{AT} = x + \ell_{t3}$$

$$y_{AT} = y + R$$

$$z_{AT} = z$$

The particular segment of the flight path is determined from the angle β where

$$\beta = \tan^{-1} \frac{y_{AT}}{z_{AT}} \frac{180}{\pi} \qquad (-360^{o} < \beta \leqq 0^{o})$$

The lateral error between the aircraft and the path is defined as that distance along a groundpath projection vector where the vector is perpendicular to the path and passing through the aircraft position. (See fig. 3.) With this position known, the path heading and the distance to go are determined. The vertical error is calculated from aircraft altitude compared with path height as a function of distance to go. Hence, given the aircraft position and a prior defined path, the lateral error Δy, vertical error Δh, distance to go D_{tg}, and desired heading ψ_r can be determined.

The lateral and vertical deviations are suitable for a navigation-guidance system; however, for the autoland system the deviations have to be normalized or scaled in terms of glide-slope and localizer errors. The simulated ILS beam shapes are shown in figure 4. The effective beam shapes are cylindrical from point 0 to point 2, where the 64-m glide-slope error is 0.7^{o} and the 351-m localizer error is 2.5^{o} for full-scale deflections. From point 2 until touchdown the beam narrows as a function of distance to go. The normalization variables for the glide slope and localizer are constant between point 0 and point 2 where $\Delta h_{nor} = 64$ m and $\Delta y_{nor} = 351$ m, respectively. These variables decrease in value from point 2 until touchdown as a function of distance to go.

The equations used for each segment of the flight path follow.

Point 0 to point 1:

$$0^{o} \geqq \beta > -90^{o}$$

$$D_{tg} = \ell_{t3} + \pi R + x_{AT}$$

$$\psi_r = 270^o$$

$$\Delta y = -y - 2R$$

$$\Delta h = h - \left(D_{tg} + \ell_{gt}\right) \tan (GSA)$$

$$\Delta y_{nor} = 351$$

$$\Delta h_{nor} = 64$$

Point 1 to point 2:

$$-90^o \geqq \beta > -180^o$$

$$D_{tg} = \ell_{t3} + \pi R\left(1 + \frac{\beta + 90}{180}\right)$$

$$\psi_r = 360^o + \beta$$

$$\Delta y = \left(x_{AT}^{\ 2} + y_{AT}^{\ 2}\right)^{1/2} - R$$

$$\Delta h = h - \left(D_{tg} + \ell_{gt}\right) \tan (GSA)$$

$$\Delta y_{nor} = 351$$

$$\Delta h_{nor} = 64$$

Point 2 to point 3:

$$-180^o \geqq \beta > -270^o$$

$$D_{tg} = \ell_{t3} + \pi R\left(\frac{\beta + 90}{180} + 1\right)$$

$$\psi_r = 360^o + \beta$$

$$\Delta y = \left(x_{AT}^2 + y_{AT}^2\right)^{1/2} - R$$

$$\Delta h = h - \left(D_{tg} + \ell_{gt}\right) \tan (GSA)$$

$$\Delta y_{nor} = \tan (2.5^o)\left(D_{tg} + \ell_r\right)$$

$$\Delta h_{nor} = \tan (0.7^o)\left(D_{tg} + \ell_{gt}\right)$$

Point 3 to threshold:

$$-270^o \geqq \beta > -360^o$$

$$D_{tg} = -x$$

$$\psi_r = 90^o$$

$$\Delta y = y$$

$$\Delta h = h - \left(D_{tg} + \ell_{gt}\right) \tan (GSA)$$

$$\Delta y_{nor} = \tan (2.5^o)\left(D_{tg} + \ell_r\right)$$

$$\Delta h_{nor} = \tan (0.7^o)\left(D_{tg} + \ell_{gt}\right)$$

The glide-slope and localizer-error equations are

$$GSE = 0.7 \frac{\Delta h}{\Delta h_{nor}}$$

and

$$\eta = 2.5 \frac{\Delta y}{\Delta y_{nor}}$$

RESULTS AND DISCUSSION

The first attempt to fly the simulated curved approach used the basic autoland control algorithms with continuous desired track angle replacing runway heading and with the simulated glide-slope and localizer-error signals. (See figs. 5 to 8.) The simulation was flown with no regard for the deceleration requirement, and the results exhibited the problem of a path standoff error during the curved portion of the task. The problem occurred because the existing autoland system was designed for a straight-in approach and the bank angle ϕ necessary for the turn could only be generated by a nonzero localizer error. The nonzero localizer error keeps the track-angle error nulled whereas the reverse is not true. A solution was to provide the control system with the nominal bank angle required to fly the turn of radius R at the current ground speed V_g. The equation used for the calculation of the nominal bank angle was (ref. 6)

$$\phi_{nom} = -\tan^{-1}\left[\frac{(V_g)^2}{Rg}\right]$$

As shown in figure 5, ϕ_{nom} is summed with track angle and localizer errors to form a commanded bank angle ϕ_c. This signal is then combined with the actual roll attitude of the aircraft to form an error signal ϕ_{er}; the ϕ_{er} commands a change in aileron position to roll the aircraft to the correct attitude. With the addition of the ϕ_{nom} signal, the simulation was run for a 120-knot, full-flap, 3^o curved approach, and the results are shown in figure 9. It should be noted that the on-course logic (ONCOR) shown in figure 5 was not allowed to be set "true" until the short final leg. This modification prevented the switching to the long-time constant in the localizer error circuit and to the lower bank-angle limit. As shown in the figure, the aircraft followed the desired groundpath very closely. The only noticeable error occurred at the initiation of the turn.

This transient error is more pronounced in a 200-knot, zero-flap, 3^o curved approach. (See fig. 10.) This error occurred because a step input was placed into the ϕ_{nom} signal at the turn initiation. The aircraft could not follow the step; therefore, the overshoot shown in the figure occurred. To reduce this overshoot in the early stages of transition from the straight segment to the curved portion of the path, the step of ϕ_{nom} was introduced before the aircraft reached the actual point of turn initiation. The amount of time necessary to roll to the desired ϕ_{nom} is approximately equal to the nominal bank angle divided by the roll rate limit of the control system (ref. 6)

$$\Delta t = \frac{\phi_{nom}}{\dot{\phi}_{limit}}$$

The roll command is then initiated when the distance to go is equal to the distance to go at point 1 $(D_{tg,1})$ added to Δt multiplied by the groundspeed

$$D_{tg} = D_{tg,1} + (V_g \Delta t)$$

The same approach could be used for the initiation of the roll-out maneuver; however, this computation was not included since, at this point along the path for a decelerating approach, ϕ_{nom} would be smaller.

Figure 10 also shows the importance of decelerating to approach speed prior to or during the final turn. As can be seen in the figure, the control system required almost the complete turn to null the initial overshoot error. This condition occurred because bank command limit of the control system is $\pm 30^{\circ}$ whereas the nominal bank angle for this 200-knot approach was -26°; thus, only 4° of bank command was left to null the initial error. If deceleration had occurred prior to the turn, ϕ_{nom} would have only been -12° and 18° of bank command would have been left to null the overshoot.

The deceleration of the aircraft from 200 knots to the desired landing speed of 120 knots was to be accomplished during the flight path. The point at which the deceleration was to begin was chosen at a specified path distance from the runway threshold. This distance was determined by minimizing flight time in the path while still allowing the performance of a satisfactory automatic landing approach. The specified distances used were 6858 m for the 3° path and 13 904 m for the 5° path. Performance of the deceleration task required the automatic deployment of the flaps and flight spoilers and the actuation of the throttles.

The throttles were controlled by using the "Indicated Airspeed Select/Hold" circuit shown as part of figure 8. The acceleration command limit was changed from 0.61 m/sec^2 to 1.22 m/sec^2 in order to increase the deceleration capabilities for this study. Once the aircraft reached the point on the path where deceleration was to begin $(D_{tg}$ = Specified value), the desired airspeed V_{cd} was set to the desired landing speed. (This signal generated a deceleration command A_c which caused the throttles to retard continuously until a prescribed lower limit was reached. The throttles remained in the position until A_c changed sign, and then the throttles moved forward, trimming the aircraft at the desired landing speed.

The deceleration command A_c was also used to deploy the flight spoilers as speed brakes and to increase the deceleration capabilities of the aircraft. As shown in figure 11, the flight spoilers were deployed and retracted at a predetermined rate (6° per sec) as a function of A_c. It should also be noted that for safety reasons the flight spoilers are not deployed below some minimum altitude. This limit prevents a possible hardover situation

caused by a spoiler failure at a lower altitude where recovery is questionable; the limit also allows the aircraft to trim prior to the initiation of the flare maneuver.

Although the throttles and flight spoilers are being driven, the flaps are also being deployed automatically as a function of indicated airspeed. This function was designed to be consistent with recommended flap placards. (See fig. 12.)

When turn anticipation was added and a deceleration from 200 knots to 120 knots carried out, the performance in flying the prescribed flight path was improved. The time histories of figure 13 and the tabulated results in table I show that a very satisfactory curved, decelerating 3° approach can be accomplished with minor modifications to the basic automatic control systems in the perfect environment. The same is true for a 5° approach (fig. 14 and table II) under the same conditions. The modified system was then tested in the presence of moderate turbulence and wind, beam discontinuities when switching from VOR and DME to MLS guidance information, and sensor noise. Several simulation runs were made with crude approximations to these errors added into the simulation. Figures 15 and 16 and tables III and IV depict candidate 3° and 5° runs, respectively, and show that the modified system performed satisfactorily even in the presence of the disturbances listed in table V. The relatively large lateral error Δy in figure 15 and table IV was caused by the high ground speed of the aircraft. For these conditions, performing the deceleration sooner would probably be advisable.

A possible autoland configuration for curved, descending, deceleration approaches, shown in major block form in figure 17, includes the proposed modifications to the present system. These relatively minor modifications are:

(1) Coupling of the navigation-guidance computer to the flight control computers during the autoland

(2) Addition of an algorithm to the navigation-guidance package; such an addition would convert microwave landing system position information into usable glide-slope and localizer errors

(3) Replacement of the static runway heading signal with a continuous desired track signal

(4) Addition of a nominal bank-angle signal to the lateral autoland control system

(5) Addition of "turn anticipation" to path definition

(6) Addition of an automatic flight spoiler control system

(7) Addition of an automatic flap control system.

CONCLUDING REMARKS

This study was made to determine a candidate guidance-autoland control system which would functionally meet the requirement of performing a fully automatic landing approach along a curved, descending, decelerating path. Such a system was obtained by modifying the basic control laws and could be implemented, hardware interface permitting, on the research support flight system with the present onboard computers. A possible autoland configuration for curved, descending, deceleration approaches includes the proposed modifications to the present system. These relatively minor modifications are:

(1) Coupling of the navigation-guidance computer to the flight control computers during the autoland

(2) Addition of an algorithm to the navigation-guidance package; such an addition would convert microwave landing system position information into usable glide-slope and localizer errors

(3) Replacement of the static runway heading signal with a continuous desired track signal

(4) Addition of a nominal bank-angle signal to the lateral autoland control system

(5) Addition of "turn anticipation" to path definition

(6) Addition of an automatic flight spoiler control system

(7) Addition of an automatic flap control system.

Langley Research Center
National Aeronautics and Space Administration
Hampton, Va. 23665
March 4, 1976

REFERENCES

1. Reeder, John P.; Taylor, Robert T.; and Walsh, Thomas M.: New Design and Operating Techniques for Improved Terminal Area Compatibility. [Preprint] 740454, Soc. Automot. Eng., Apr.-May 1974.

2. Hoffman, William C.; Zvara, John; and Bryson, Arthur E., Jr.: A Landing Approach Guidance Scheme for Unpowered Lifting Vehicles. AIAA Paper No. 69-865, Aug. 1969.

3. Burrows, James W.; and Tobie, H. N.: Linear Energy Management During Unpowered Landing Approach. Doc. No. D6-24909TN, Boeing Co., [1971].

4. Crawford, Daniel J.; and Bowles, Roland L.: Automatic Guidance and Control of a Transport Aircraft During a Helical Landing Approach. NASA TN D-7980, 1975.

5. Reeder, John P.: Future Airborne Systems for Terminal Area Operations. Paper Presented at the 18th Symposium of the Society of Experimental Test Pilots, Sept. 1974.

6. McKinstry, R. Gill: Guidance Algorithms and Non-Critical Control Laws for ADEDS and the AGCS. Model NASA 515. Doc. D6-41565, Boeing Co., 1974.

7. Bjurman, B. E.; Jones, D. L.; McKinstry, R. G.; and O'Toole, P. L.: Supplemental Flight Test Report. Doc. D6-41593, Boeing Co., 1974.

8. Salmirs, Seymour; and Tobie, Harold N.: Electronic Displays and Digital Automatic Control in Advanced Terminal Area Operations. AIAA Paper No. 74-27, Jan.-Feb. 1974.

9. Grove, Randall D.; and Mayhew, Stanley C.: A Real-Time Digital Program for Estimating Aircraft Stability and Control Parameters From Flight Test Data by Using the Maximum Likelihood Method. NASA TM X-2788, 1973.

TABLE I.- CURVED PATH RESULTS FOR 3° GLIDE SLOPE

Path distance to threshold, D_{tg}, m	Lateral error, Δy, m	Vertical error, Δh, m	Calibrated airspeed, V_c, knots	Pitch attitude, θ, deg	Flap position, δ_F, deg	Roll attitude, ϕ, deg	Vertical speed, h, m/sec	Track error, $\Delta\psi_{tr}$, deg
13 904	152.40	-134.11	205.8	3.8	2.5	0.0	0.00	0.0
8 418	-5.79	.85	205.0	1.1	2.3	-10.9	-5.50	-2.4
4 971	16.06	.49	187.2	2.9	7.6	-22.5	-5.18	-.3
1 524	1.37	-5.43	127.1	-0.0	40.0	-11.3	-3.23	-.1
1 219	-11.12	-4.32	123.9	1.1	40.0	6.7	-2.86	-2.3
914	-12.92	-2.66	122.8	.4	40.0	1.7	-3.25	1.3
610	-5.97	-2.57	122.1	.6	40.0	-2.2	-3.20	.8
305	-5.12	-2.47	121.6	.5	40.0	0.0	-3.29	-.4
0	-4.21	-2.72	121.2	.9	40.0	1.4	-3.32	.9

TABLE II.- CURVED PATH RESULTS FOR 5° GLIDE SLOPE

Path distance to threshold, D_{tg}, m	Lateral error, Δy, m	Vertical error, Δh, m	Calibrated airspeed, V_c, knots	Pitch attitude, θ, deg	Flap position, δ_F, deg	Roll attitude, ϕ, deg	Vertical speed, h, m/sec	Track error, $\Delta\psi_{tr}$, deg
13 904	152.40	-23.77	212.1	3.5	2.5	0.0	-0.04	0.0
8 418	-46.02	-8.23	189.1	.9	8.8	-11.3	-8.69	-3.3
4 971	4.27	-4.27	162.0	-.6	29.2	-18.2	-6.61	-.5
1 524	3.35	-.61	122.1	-1.0	40.0	-10.8	-5.39	-.1
1 219	-8.53	-.61	121.6	-.7	40.0	4.5	-5.21	-2.4
914	-13.41	-.61	121.8	-1.5	40.0	3.8	-5.61	.6
610	-5.18	-.61	121.7	-1.2	40.0	-.5	-5.43	1.9
305	.30	-.61	121.4	-1.3	40.0	-2.5	-5.46	-.2
0	-3.05	-.61	121.1	-1.3	40.0	1.7	-5.43	-.4

TABLE III.- CURVED PATH RESULTS FOR 3° GLIDE SLOPE WITH DISTURBANCES

Path distance to threshold, D_{tg}, m	Lateral error, Δy, m	Vertical error, Δh, m	Calibrated airspeed, V_c, knots	Pitch attitude, θ, deg	Flap position, δ_F, deg	Roll attitude, ϕ, deg	Vertical speed, $\dot{h}$, m/sec	Track error, $\Delta\psi_{tr}$, deg
13 904	152.40	-134.11	205.7	3.8	2.5	0.0	0.00	0.0
8 418	-74.98	18.29	202.0	.2	3.0	-9.5	-5.79	-1.8
4 971	272.19	-9.14	186.2	3.2	5.2	-29.4	-4.18	-.6
1 524	10.67	-1.22	120.5	2.3	40.0	-7.6	-2.26	-.6
1 219	-.91	.30	121.4	1.1	40.0	4.2	-2.77	-1.7
914	-1.52	.91	121.4	.4	40.0	-1.0	-2.90	.7
610	-.46	-.30	118.7	1.7	40.0	-.1	-2.77	-.4
305	-2.13	.30	119.0	1.3	40.0	-.8	-2.68	-.3
0	-.65	.30	119.0	1.4	40.0	.3	-2.71	.3

TABLE IV.- CURVED PATH RESULTS FOR 5° GLIDE SLOPE WITH DISTURBANCES

Path distance to threshold, D_{tg}, m	Lateral error, Δy, m	Vertical error, Δh, m	Calibrated airspeed, V_c, knots	Pitch attitude, θ, deg	Flap position, δ_F, deg	Roll attitude, ϕ, deg	Vertical speed, $\dot{h}$, m/sec	Track error, $\Delta\psi_{tr}$, deg
13 904	152.40	-23.77	211.9	3.8	2.5	0.0	0.00	0.0
8 418	-12.80	-17.07	198.0	.3	4.6	-10.6	-10.00	-1.9
4 971	11.28	-6.10	168.9	1.4	20.5	-17.4	-7.47	-1.1
1 524	2.13	-1.52	121.4	-.6	40.0	-8.9	-5.06	.4
1 219	-6.71	-1.22	122.0	-.9	40.0	4.8	-4.91	-1.4
914	-4.27	-.91	122.3	-.8	40.0	-1.4	-4.85	1.4
610	2.44	-.91	119.8	-.1	40.0	-1.4	-4.97	.2
305	-.91	-1.22	119.5	-.1	40.0	.8	-4.57	-.3
0	-.91	-.61	120.3	-.2	40.0	0.0	-4.39	0.0

TABLE V.- DISTURBANCES USED FOR CURVED PATH

Glide slope, deg	Navigation noise, standard deviation, deg	MLS noise, standard deviation, deg	Discontinuity in glide slope at point 1, deg	Discontinuity in localizer at point 1, deg	Turbulence, standard deviation, m/deg	Wind magnitude, mean, deg	Wind heading, deg
3	0.02	0.01	-0.2	0.5	0.76	7.6	90
5	.02	.01	.05	.1	.76	7.6	90

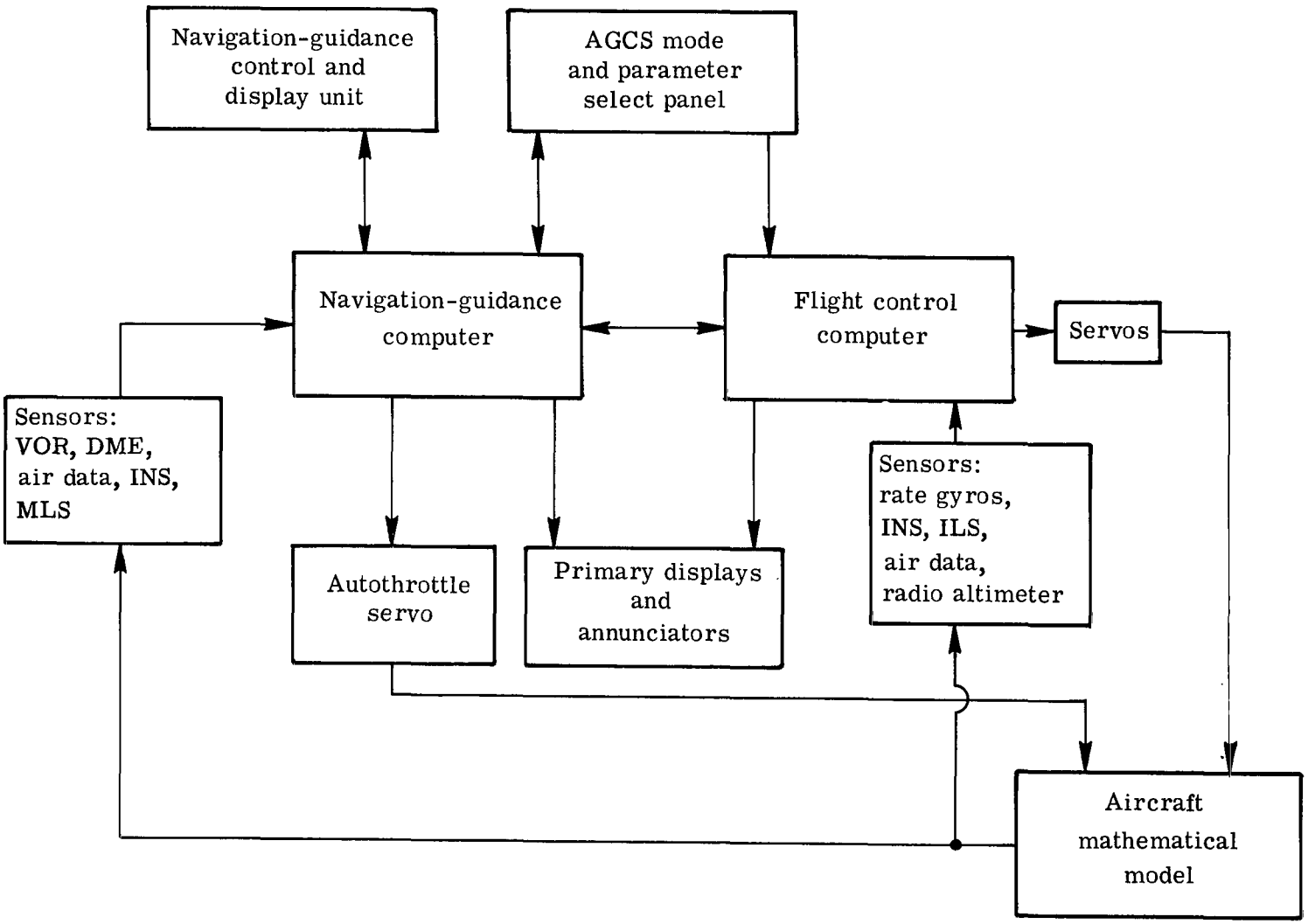

Figure 1.- Major components of research support flight system simulation.

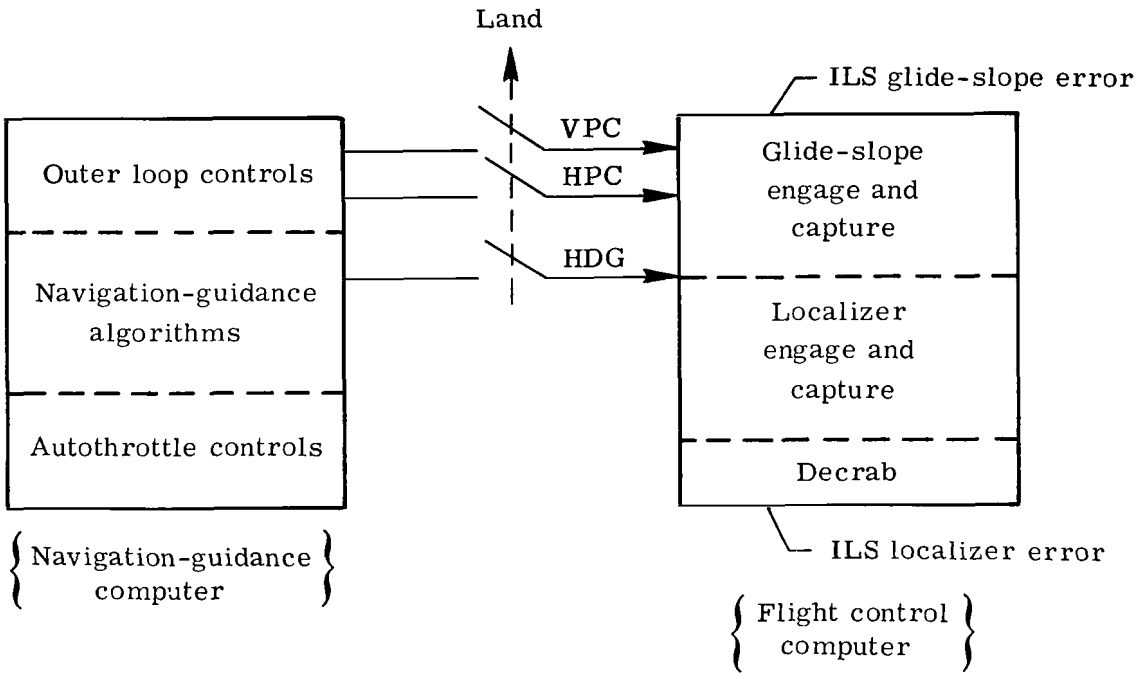

Figure 2.- Basic autoland configuration.

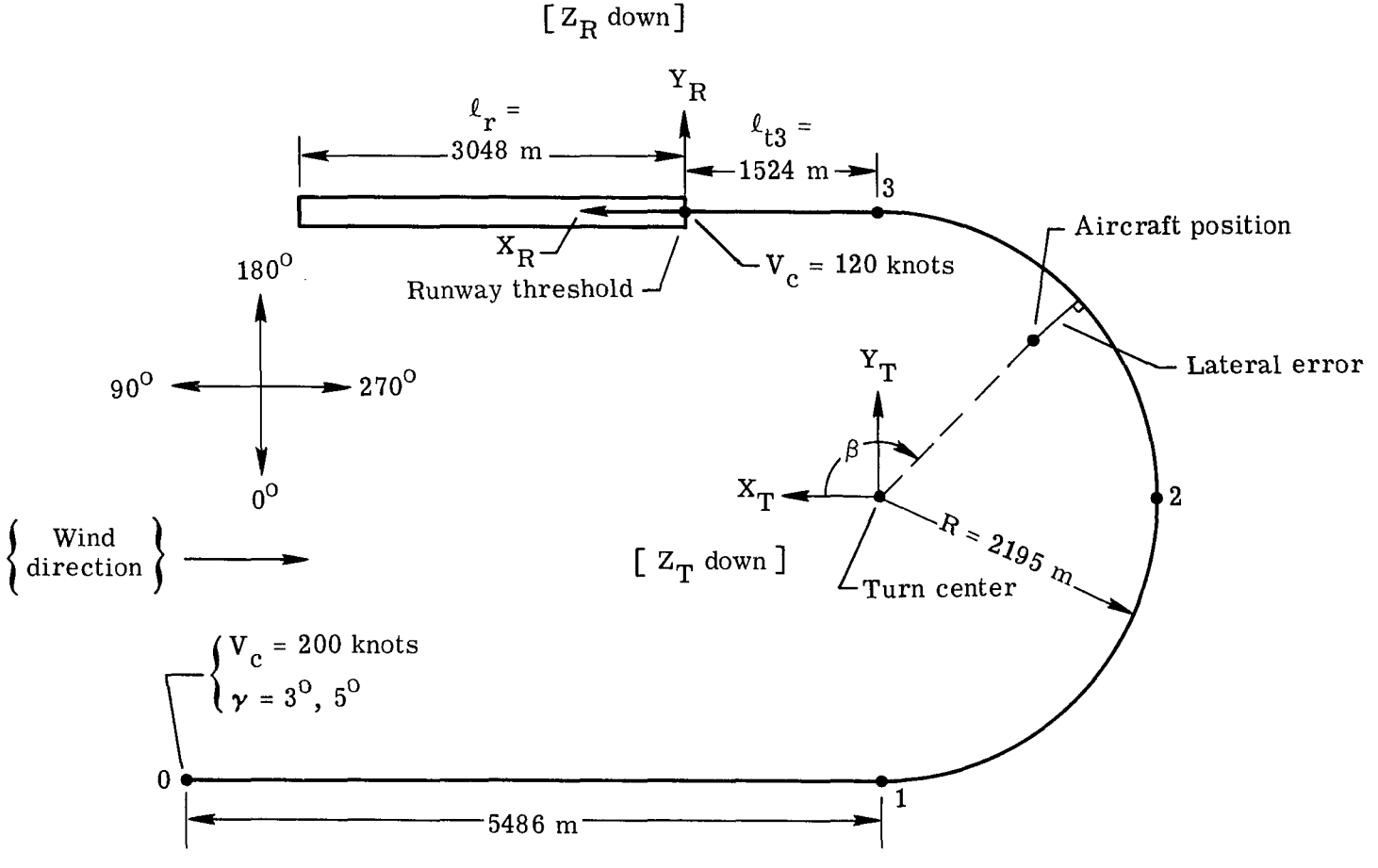

Figure 3.- Curved, descending, decelerating flight path.

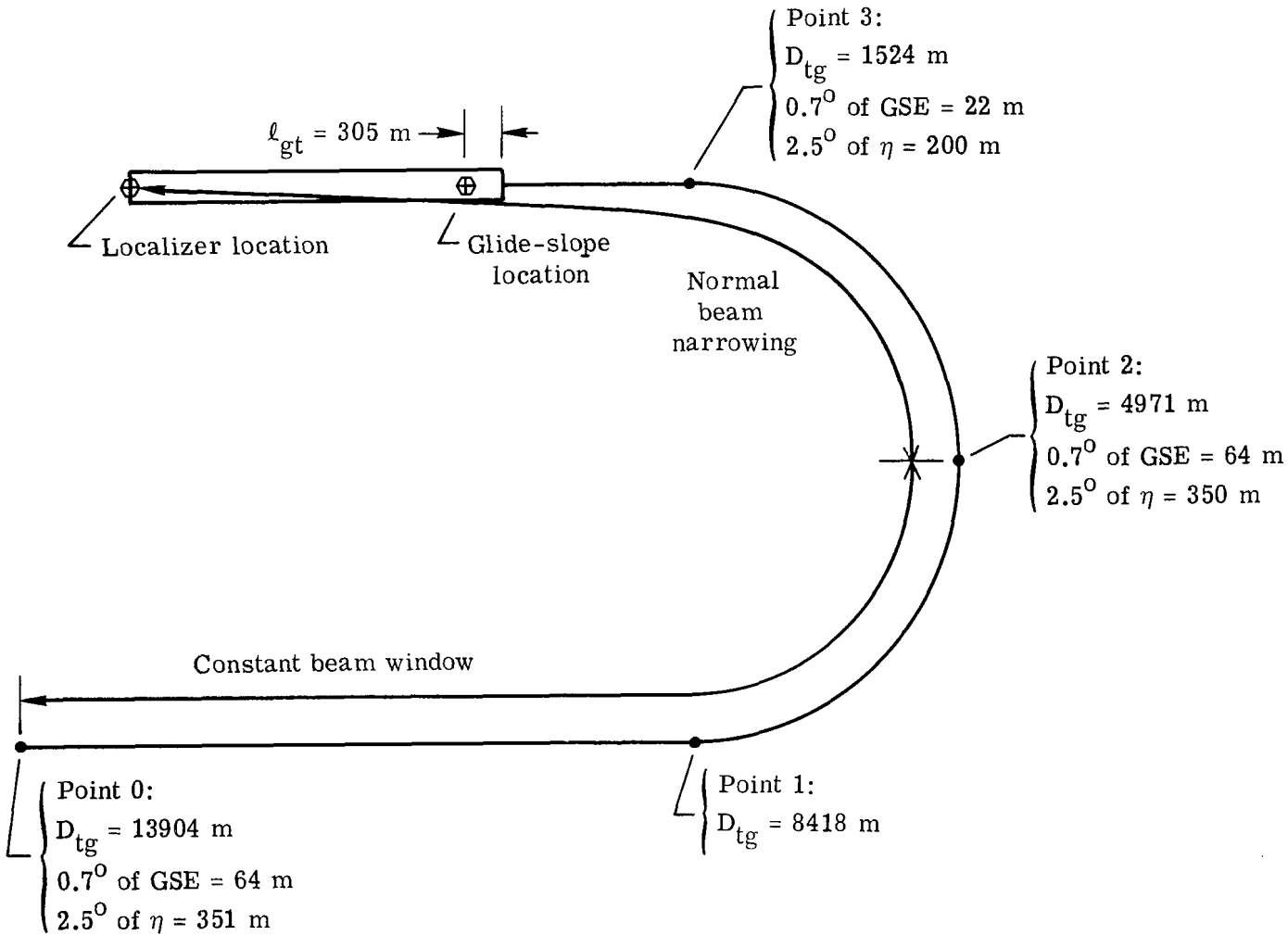

Figure 4.- Equivalent instrument landing system beam shapes.

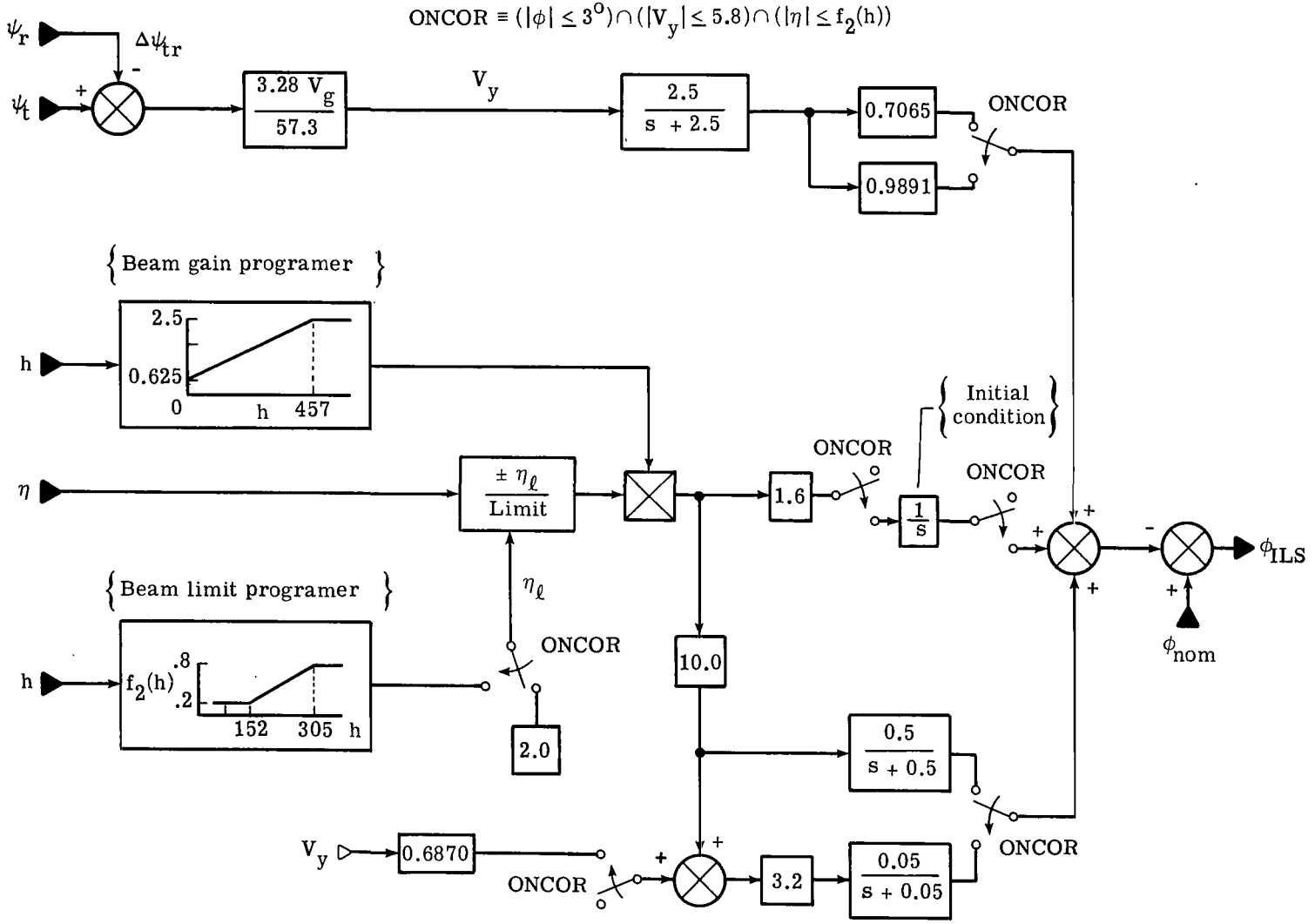

(a) Lateral error signal.

Figure 5.- Lateral autoland circuit.

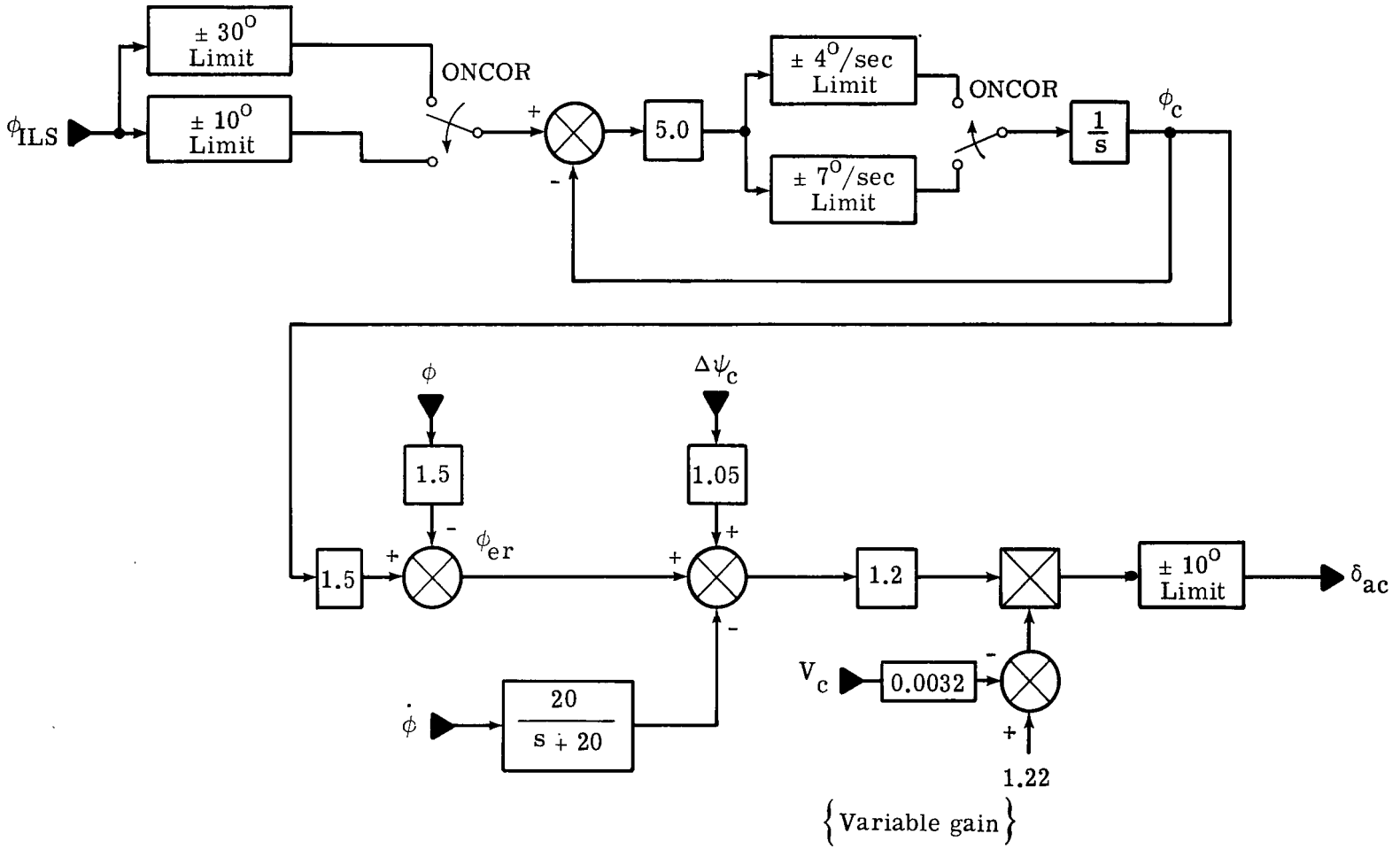

(b) Aileron command signal.

Figure 5.- Concluded.

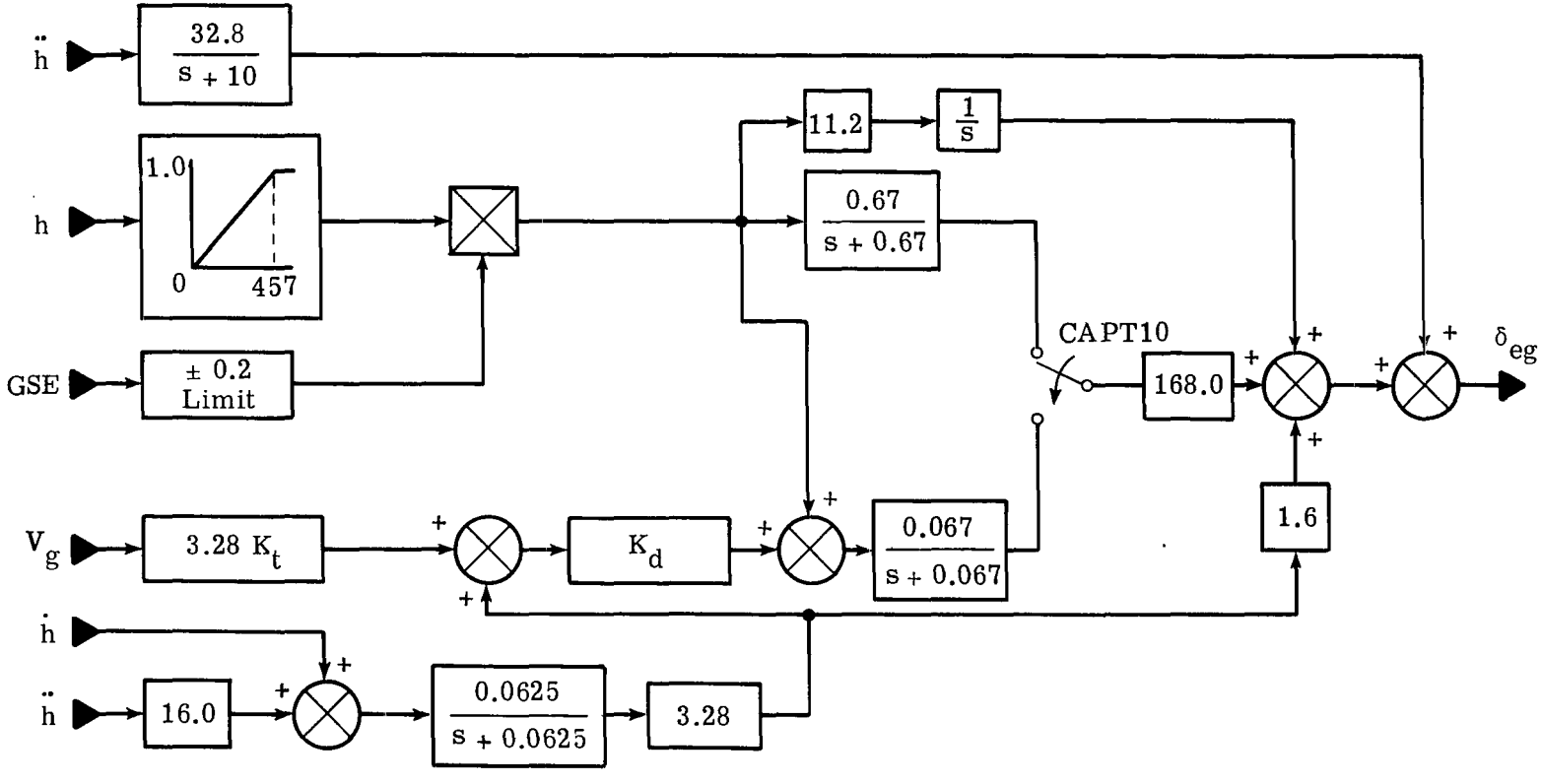

(a) Longitudinal error signal.

Figure 6.- Longitudinal autoland circuit; CAPT10 ≡ 10 sec after ($|GSE| \leq 0.108$).

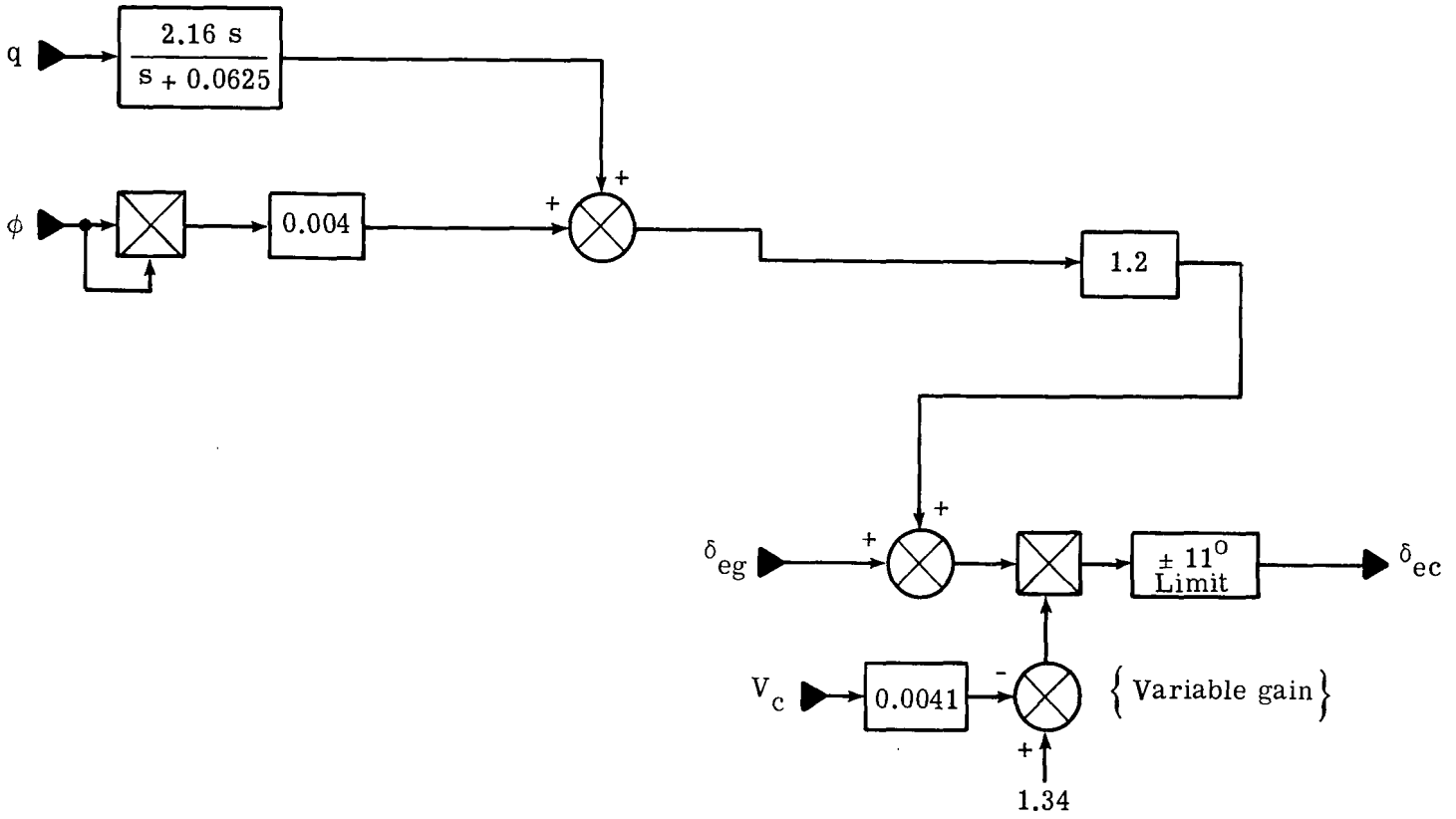

(b) Elevator command signal.

Figure 6.- Concluded.

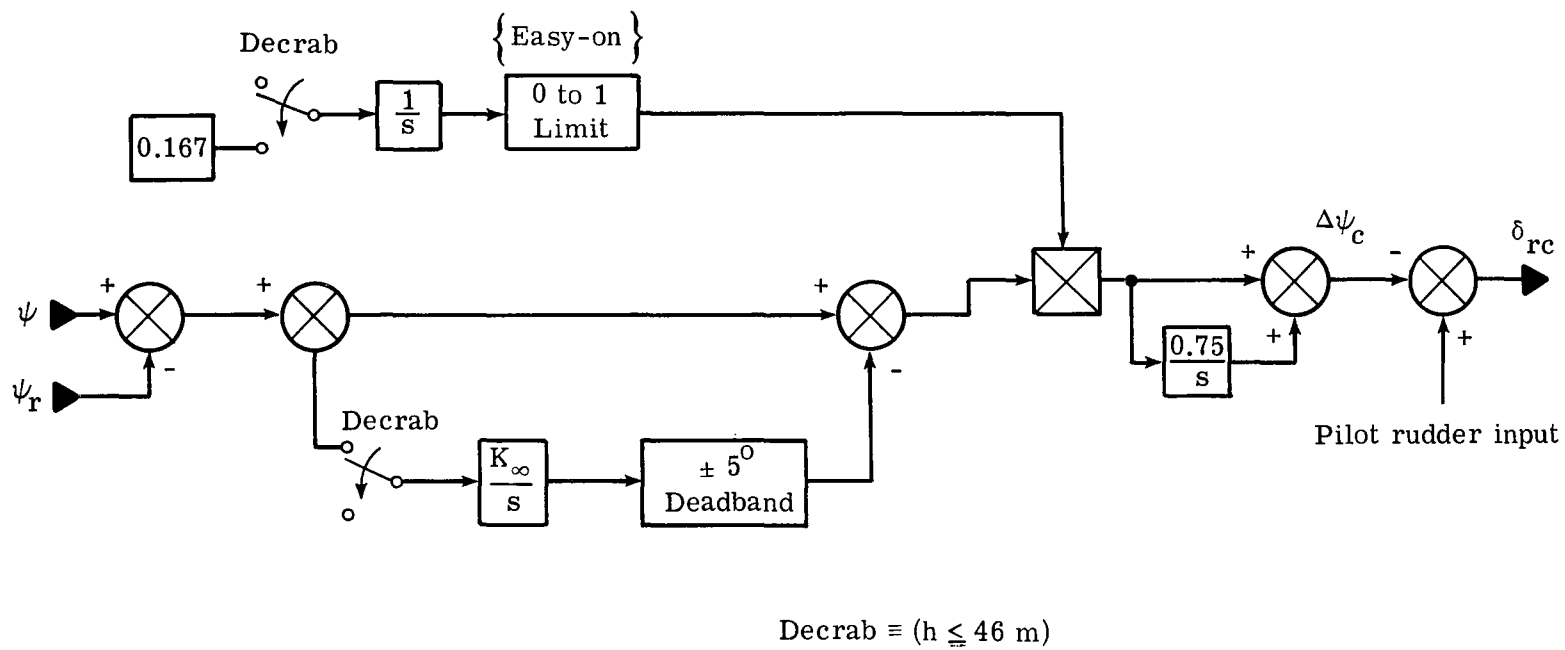

Decrab ≡ (h ≤ 46 m)

Figure 7.- Decrab circuit. Circuit including K_∞/s represents a track-hold function.

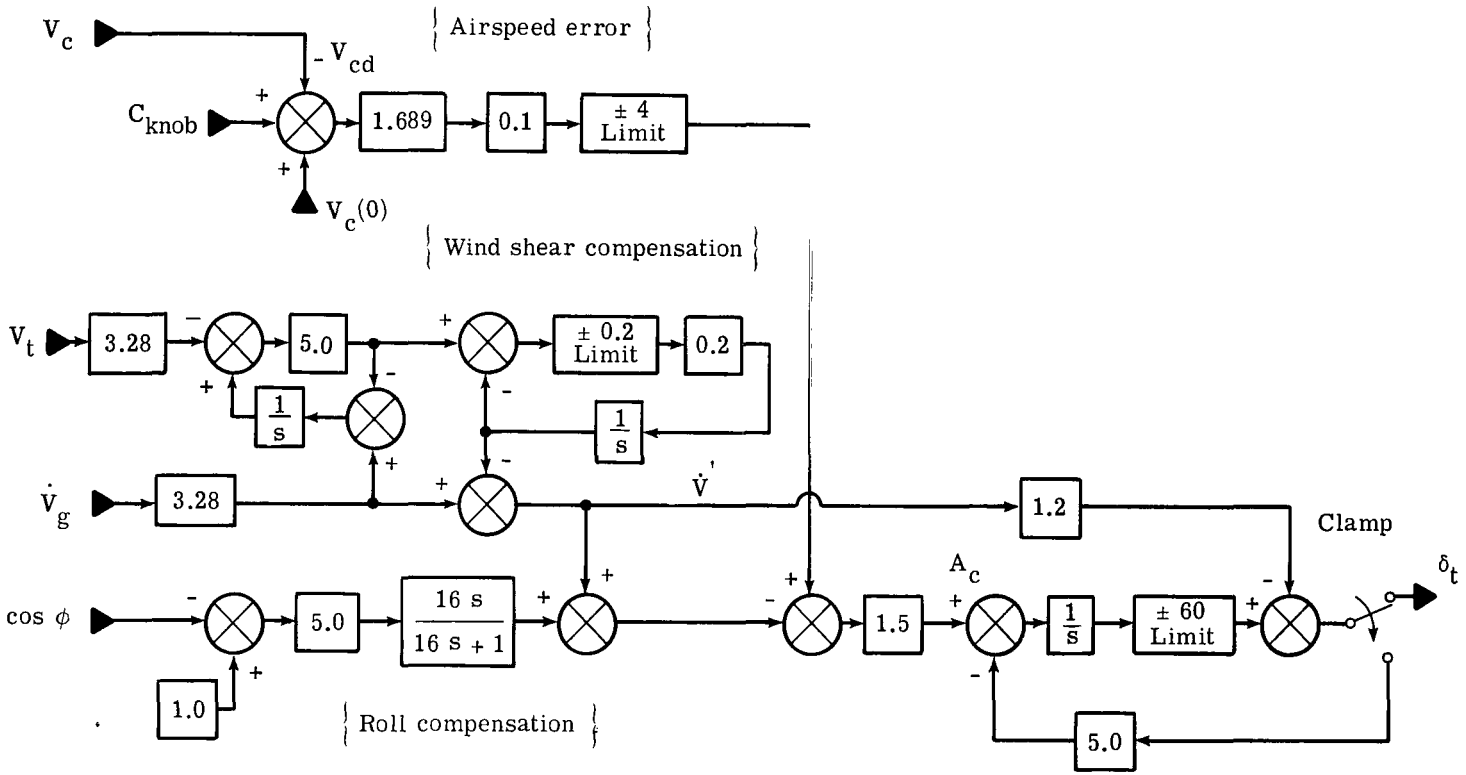

Clamp = $(A_c < 0) \cap$ (Throttle position $\leq 10^0$)

Figure 8.- Autothrottle circuit during indicated airspeed select/hold mode.

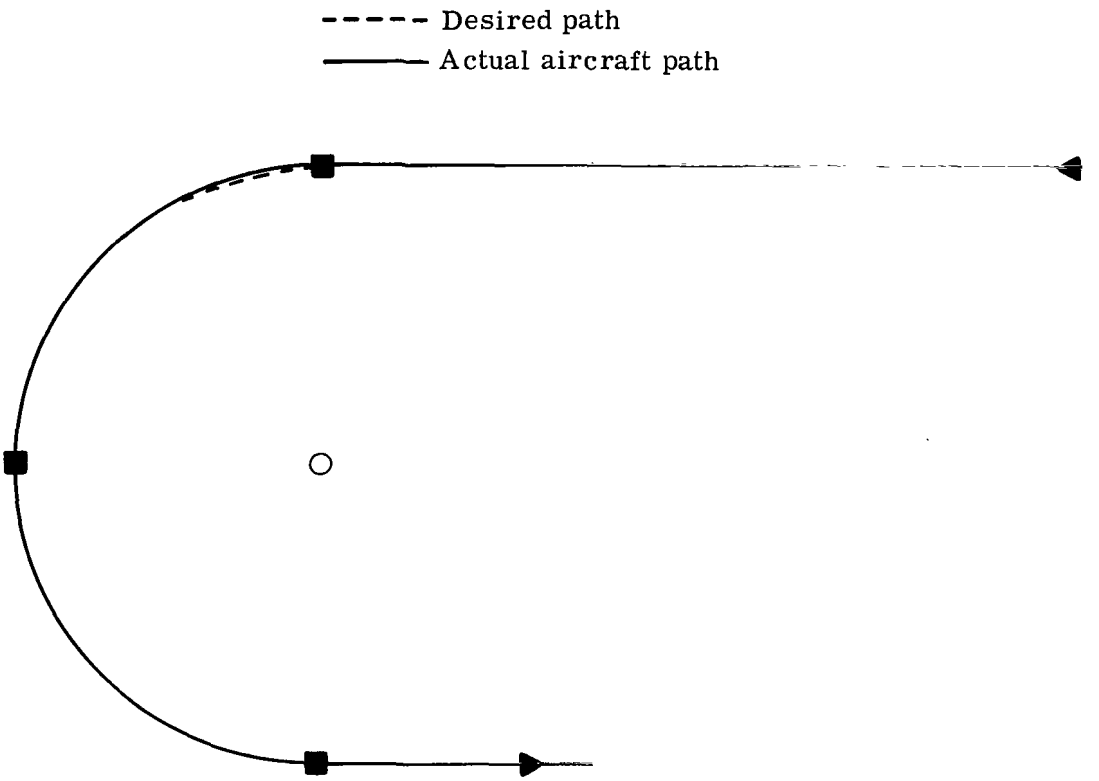

Figure 9.- Ground track for 3^{o} glidepath at 120 knots using control system without "turn anticipation."

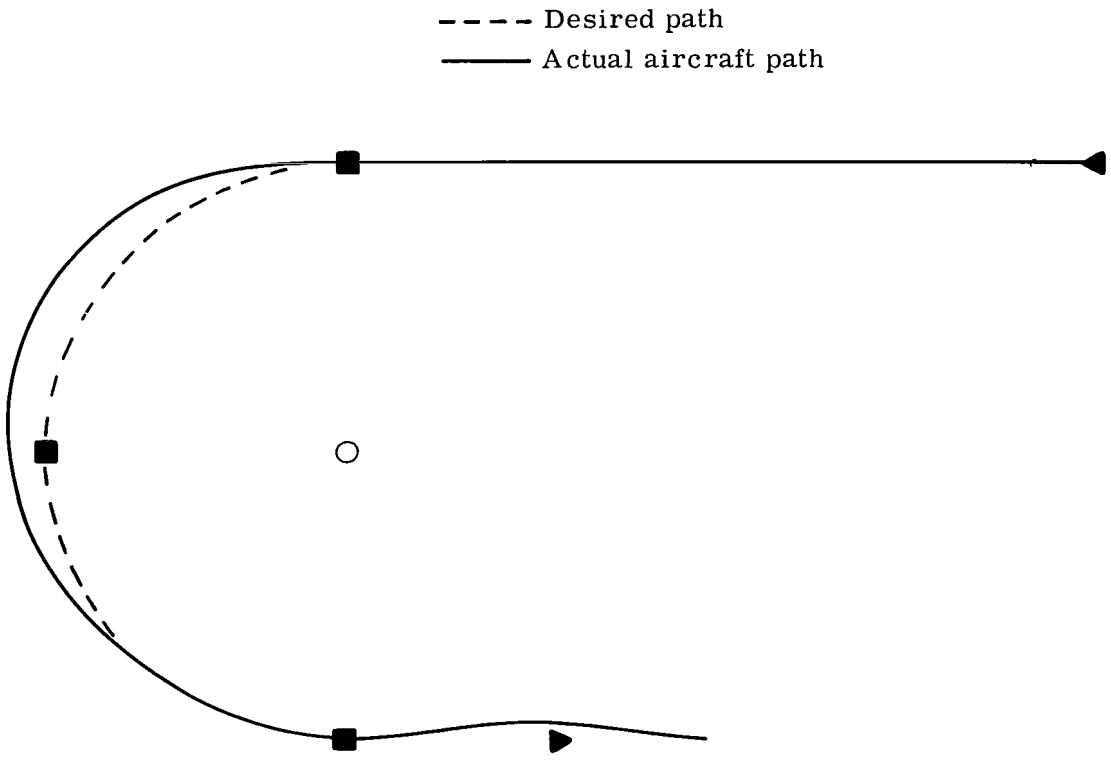

Figure 10.- Ground track for 3^{o} glidepath at 200 knots using control system without "turn anticipation."

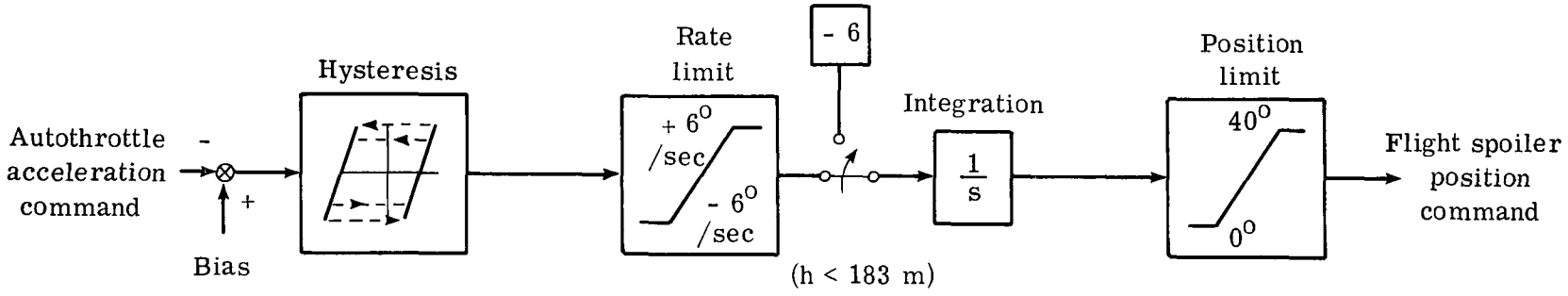

Figure 11.- Automatic flight spoiler circuit.

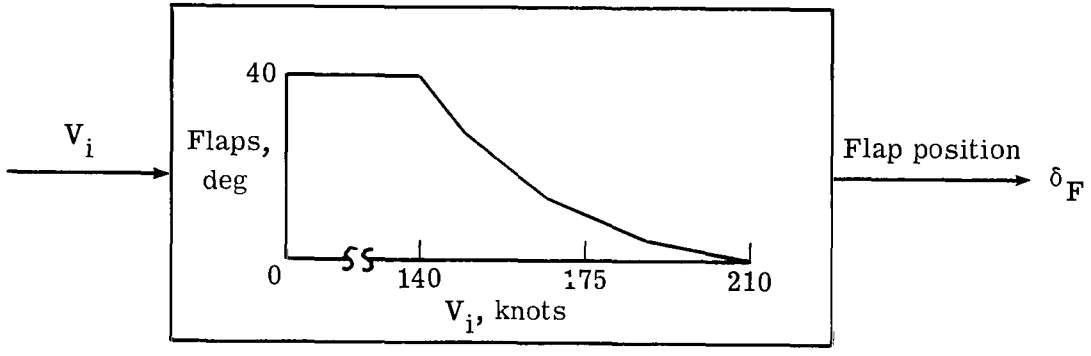

Figure 12.- Open loop automatic flap circuit.

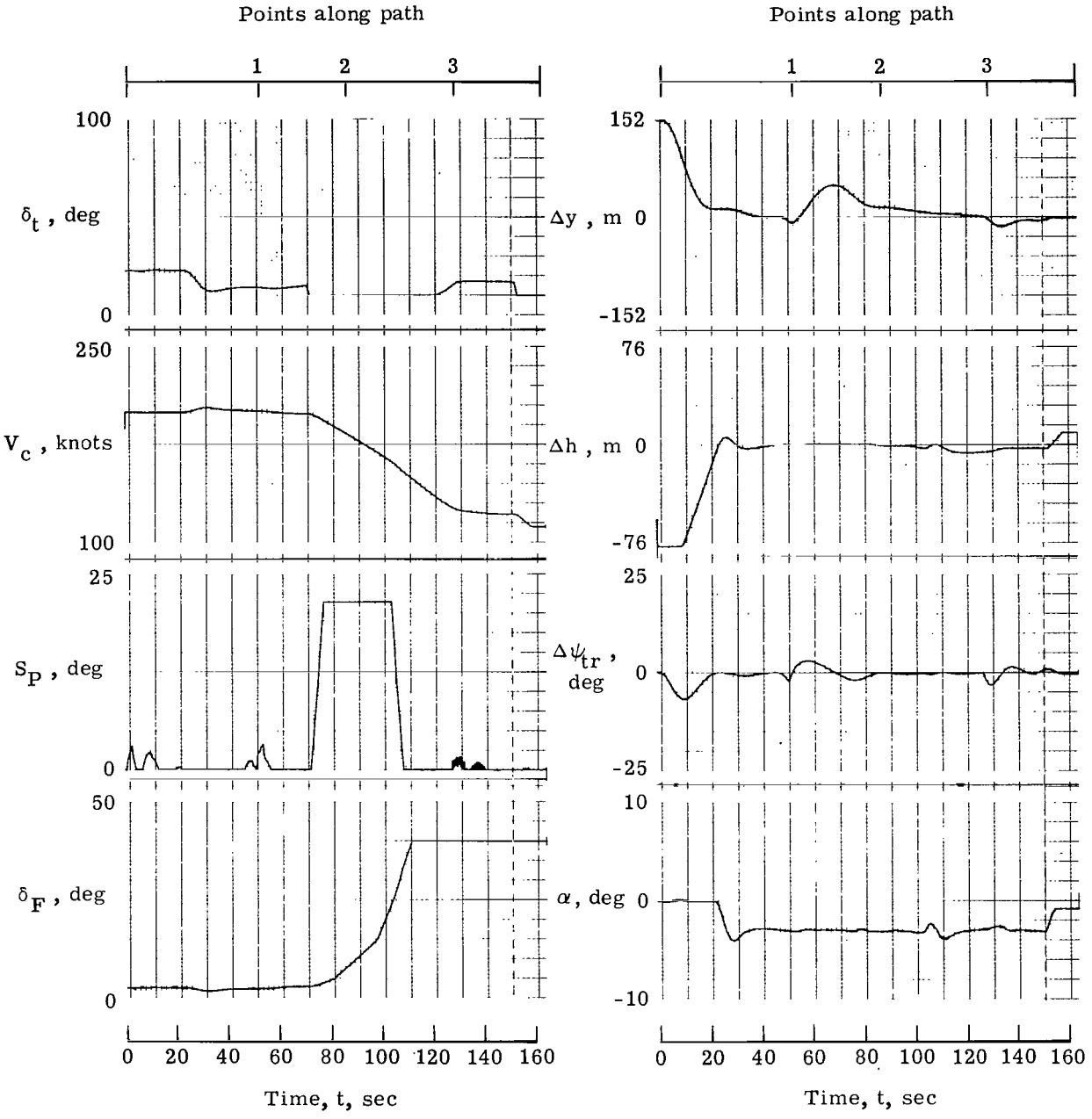

(a) Deceleration task variables.

(b) Performance variables.

Figure 13.- Aircraft-performance and control variables for 3° glide slope using modified control system.

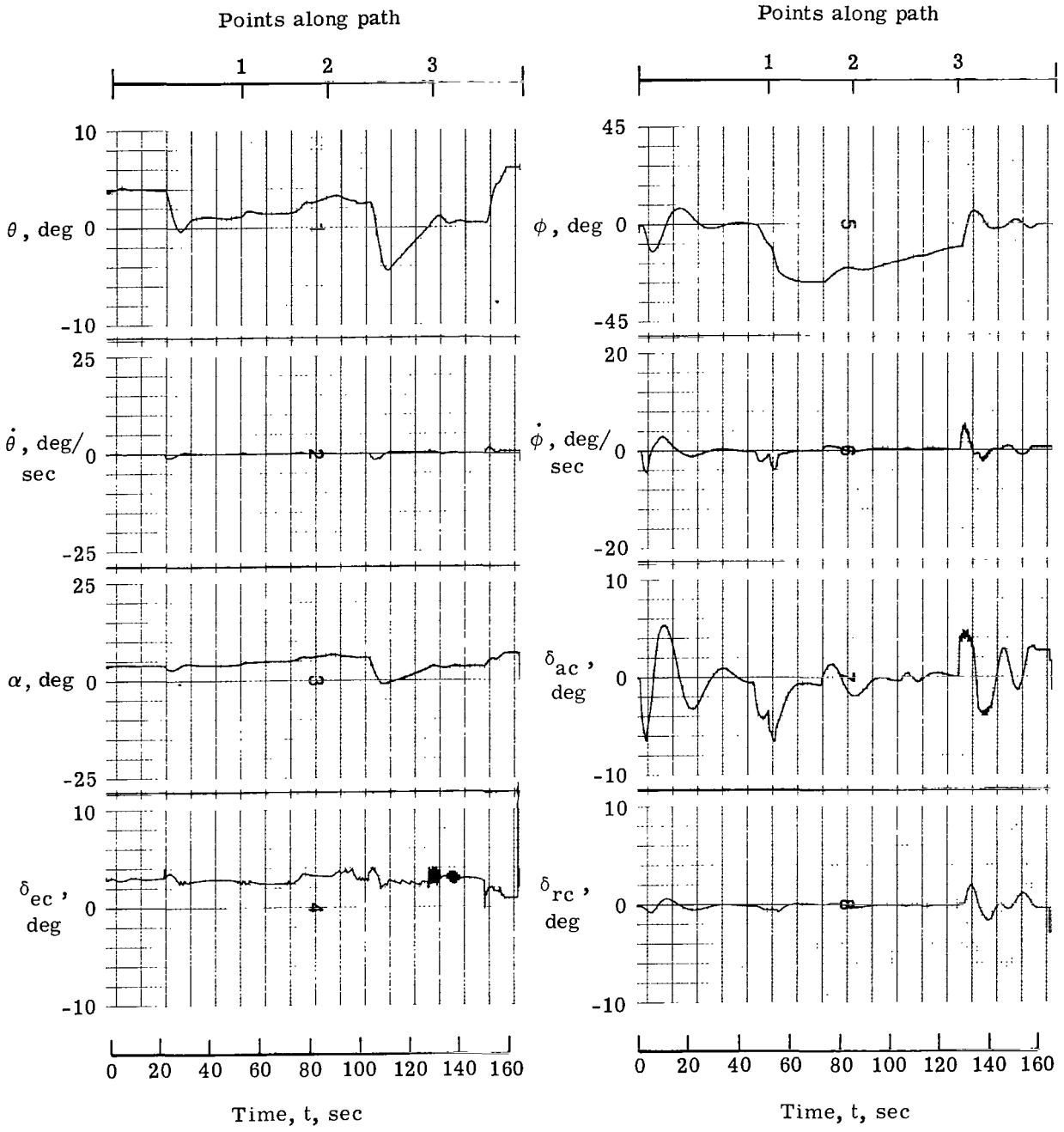

(c) Aircraft flight and control variables.

Figure 13.- Concluded.

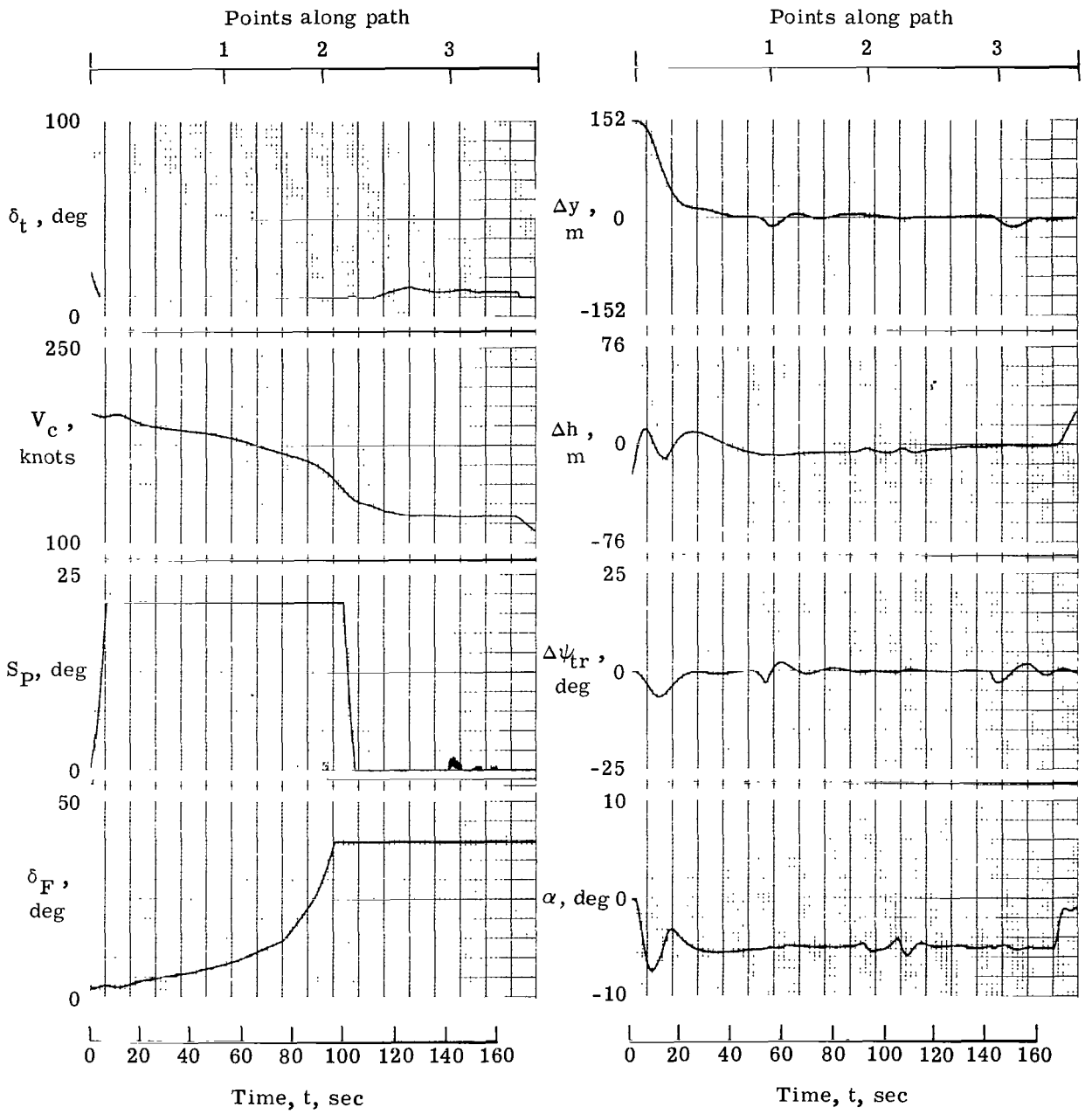

(a) Deceleration task variables.

(b) Performance variables.

Figure 14.- Aircraft-performance and control variables for 5° glide slope using modified control system.

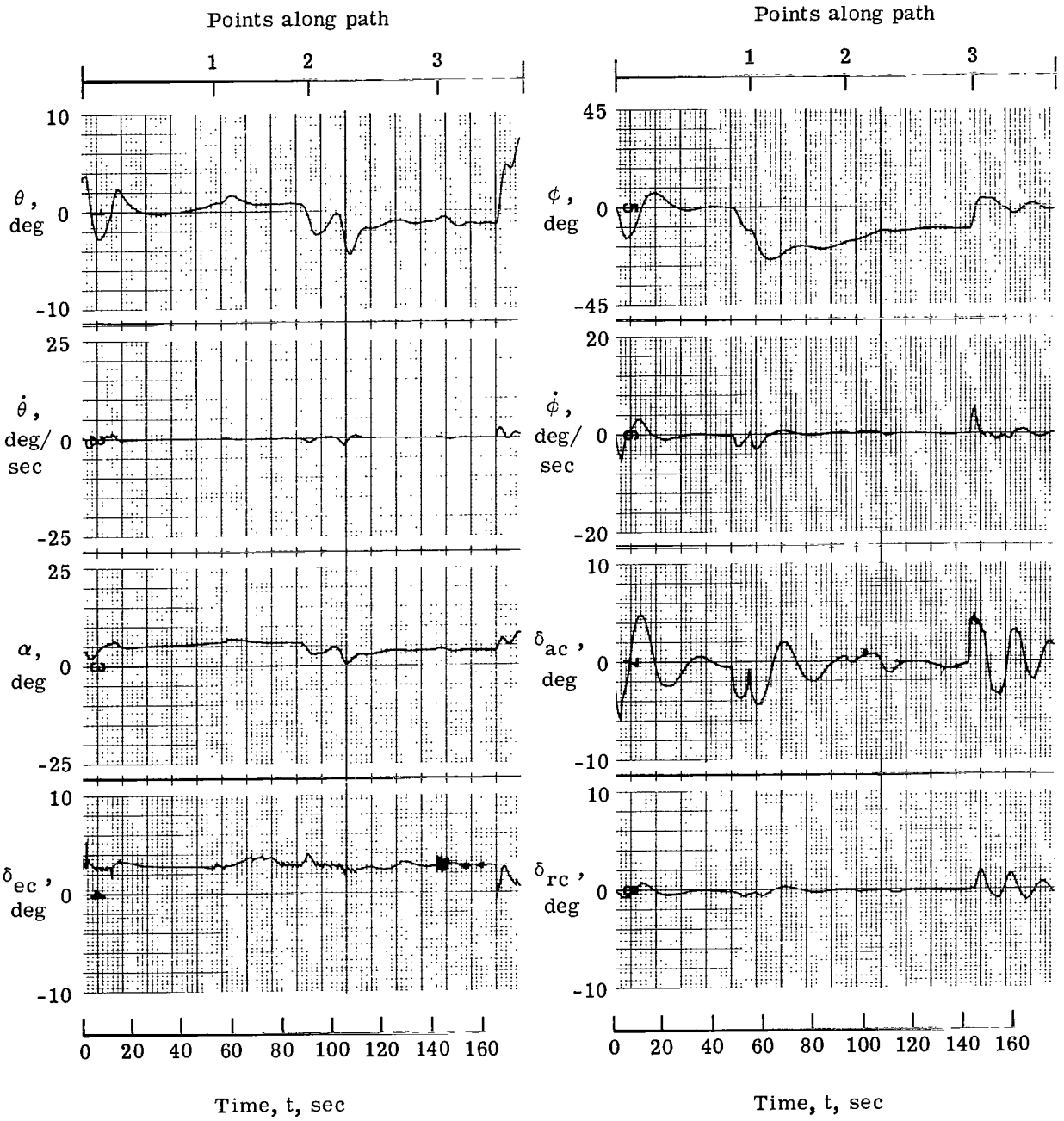

(c) Aircraft flight and control variables.

Figure 14.- Concluded.

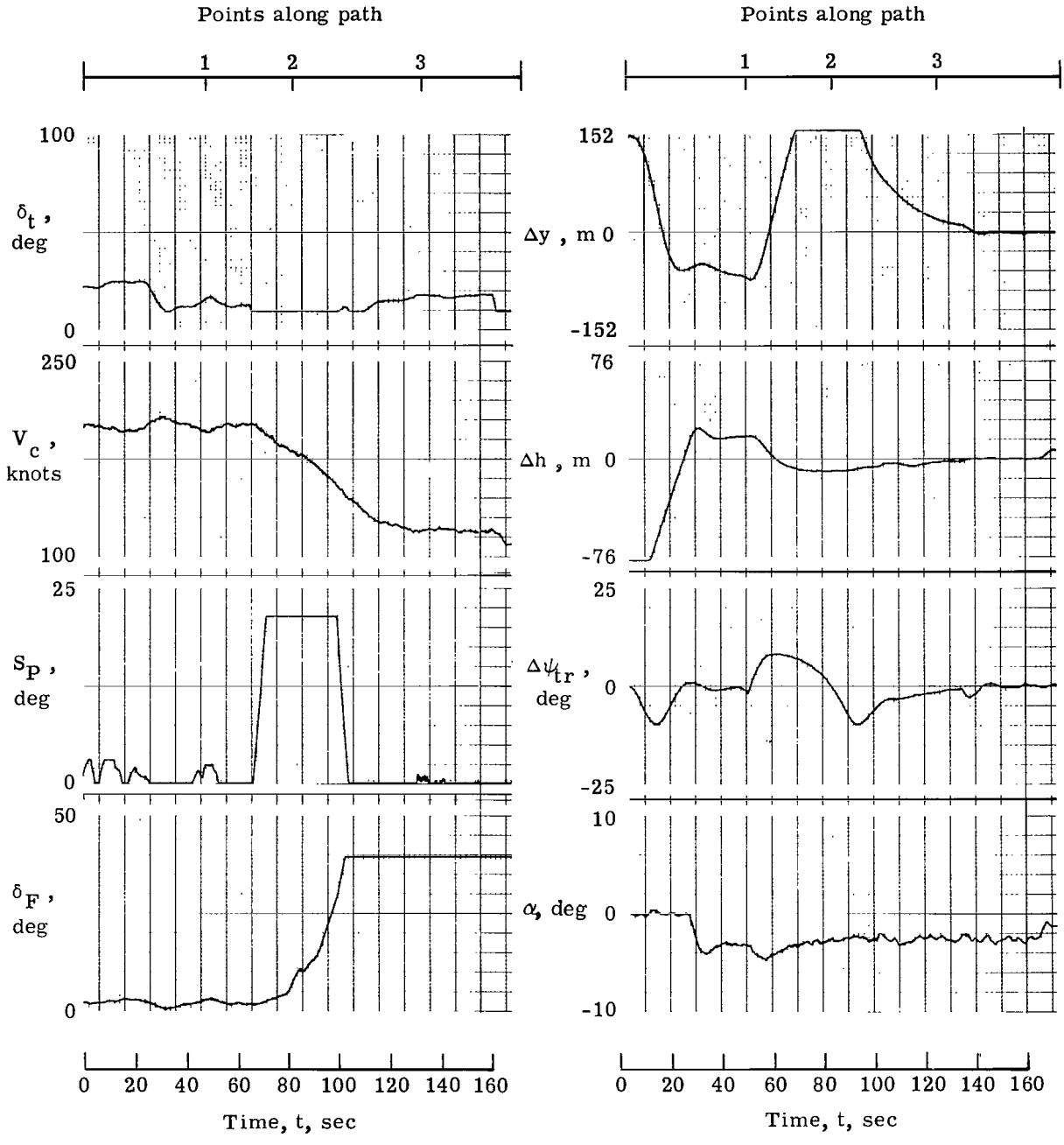

(a) Deceleration task variables.

(b) Performance variables.

Figure 15.- Aircraft-performance and control variables for 3° glide slope with disturbances using modified control system.

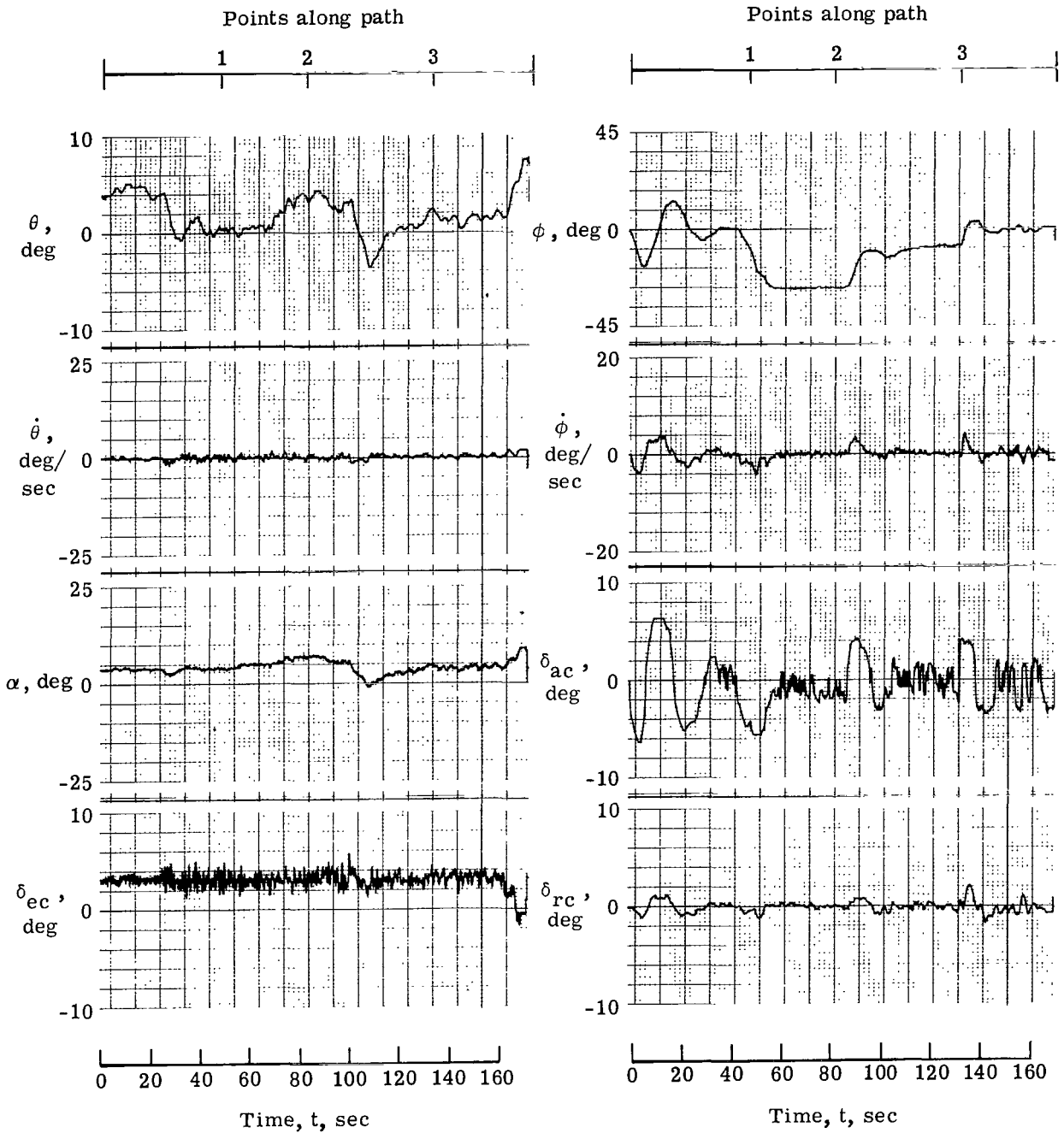

(c) Aircraft flight and control variables.

Figure 15. - Concluded.

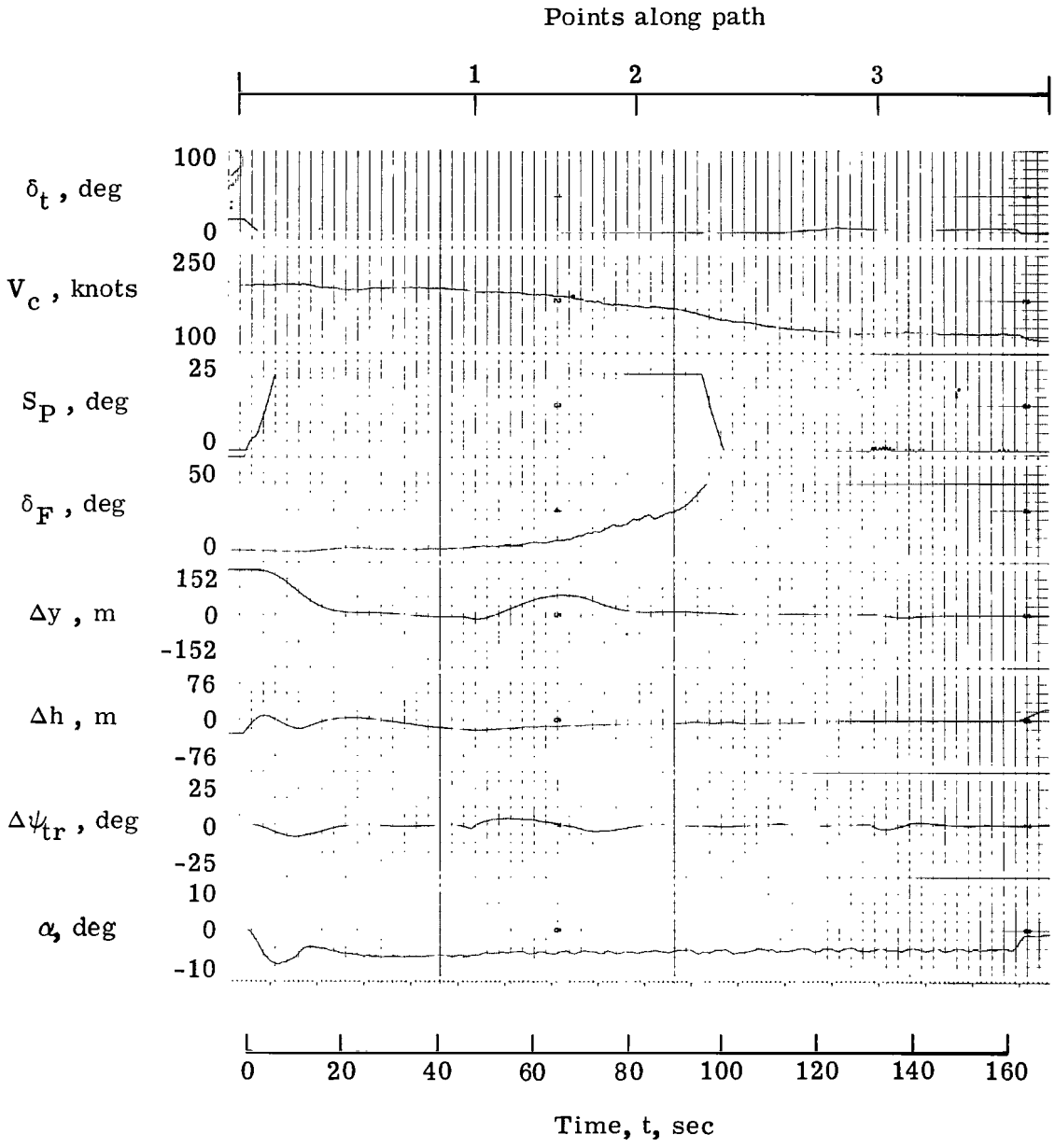

(a) Deceleration and performance variables.

Figure 16.- Aircraft-performance and control variables for 5° glide slope with disturbances using modified control system.

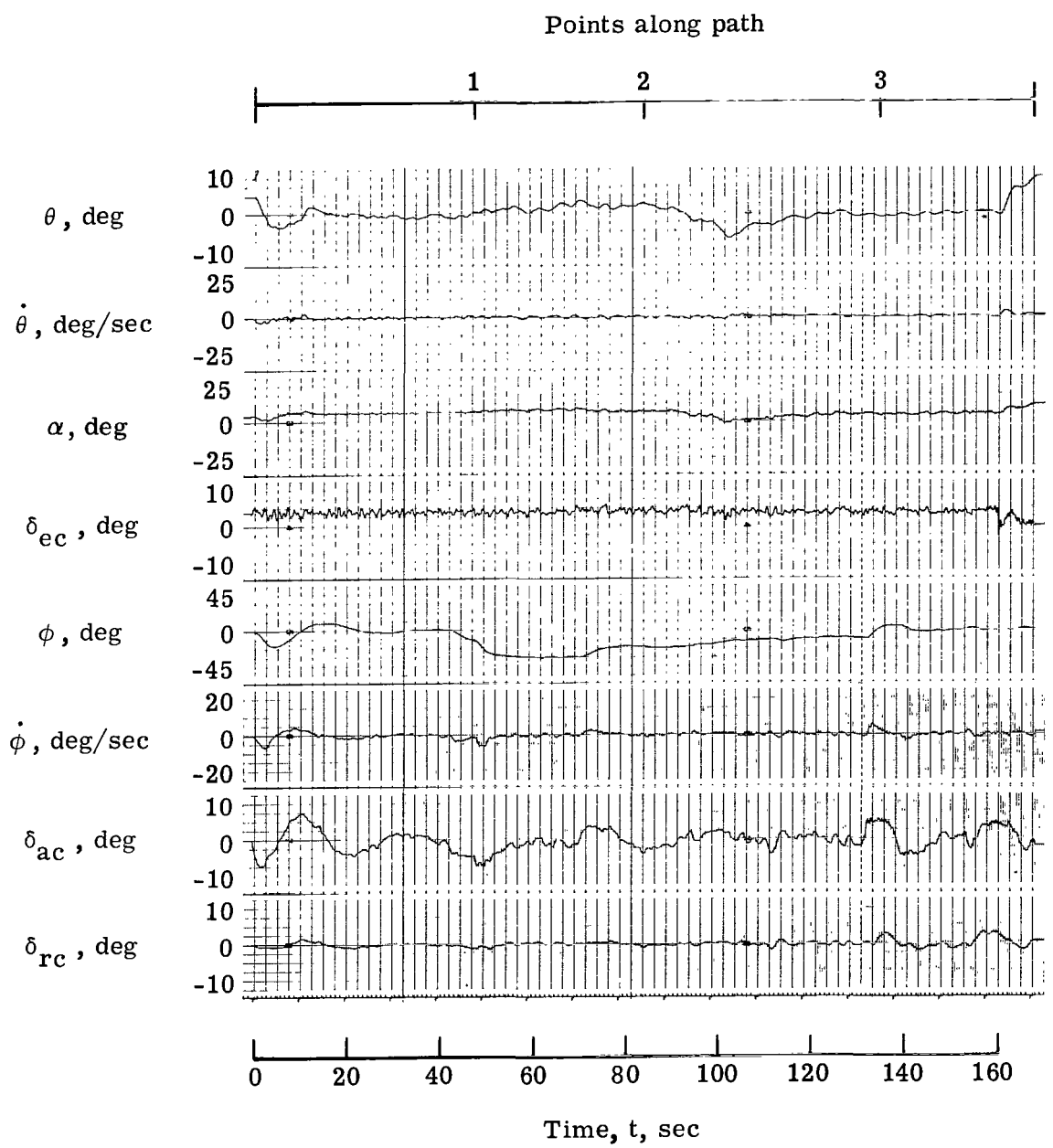

(b) Aircraft flight and control variables.

Figure 16.- Concluded.

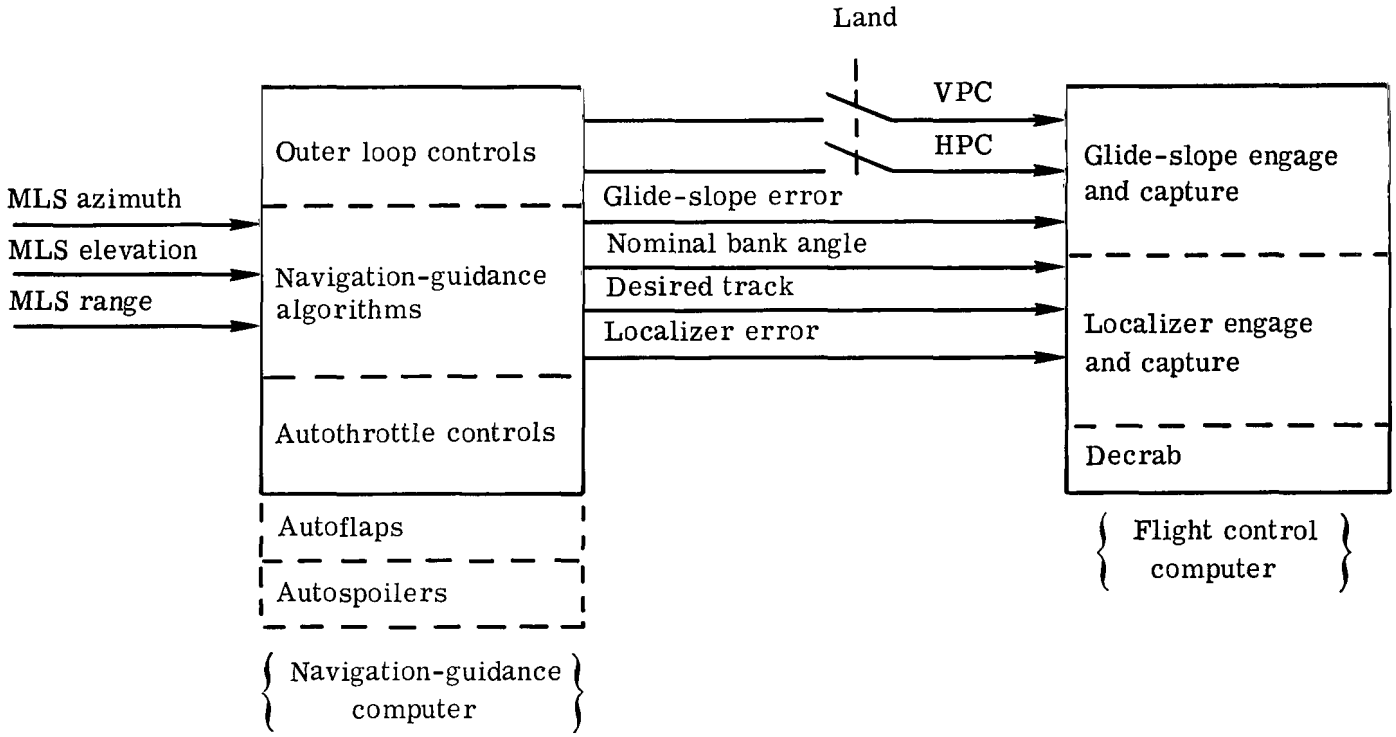

Figure 17.- Autoland configuration modified for curved, descending, decelerating approaches.

"The aeronautical and space activities of the United States shall be conducted so as to contribute . . . to the expansion of human knowledge of phenomena in the atmosphere and space. The Administration shall provide for the widest practicable and appropriate dissemination of information concerning its activities and the results thereof."

—NATIONAL AERONAUTICS AND SPACE ACT OF 1958

NASA SCIENTIFIC AND TECHNICAL PUBLICATIONS

TECHNICAL REPORTS: Scientific and technical information considered important, complete, and a lasting contribution to existing knowledge.

TECHNICAL NOTES: Information less broad in scope but nevertheless of importance as a contribution to existing knowledge.

TECHNICAL MEMORANDUMS: Information receiving limited distribution because of preliminary data, security classification, or other reasons. Also includes conference proceedings with either limited or unlimited distribution.

CONTRACTOR REPORTS: Scientific and technical information generated under a NASA contract or grant and considered an important contribution to existing knowledge.

TECHNICAL TRANSLATIONS: Information published in a foreign language considered to merit NASA distribution in English.

SPECIAL PUBLICATIONS: Information derived from or of value to NASA activities. Publications include final reports of major projects, monographs, data compilations, handbooks, sourcebooks, and special bibliographies.

TECHNOLOGY UTILIZATION PUBLICATIONS: Information on technology used by NASA that may be of particular interest in commercial and other non-aerospace applications. Publications include Tech Briefs, Technology Utilization Reports and Technology Surveys.

Details on the availability of these publications may be obtained from:

SCIENTIFIC AND TECHNICAL INFORMATION OFFICE

NATIONAL AERONAUTICS AND SPACE ADMINISTRATION

Washington, D.C. 20546